Bulletin of Volcanology (2021) 83: 28
https://doi.org/10.1007/s00445-021-01449-0

RESEARCH ARTICLE

Late Holocene Malpaís de Zacapu (Michoacán, Mexico) andesitic lava flows: rheology and eruption properties based on LiDAR image

Nanci Reyes-Guzmán[1] · Claus Siebe[1] · Magdalena Oryaëlle Chevrel[2] · Gregory Pereira[3]

Received: 13 August 2020 / Accepted: 5 March 2021 / Published online: 30 March 2021

Abstract
Few monogenetic eruptions that produced lava flows have occurred in historical times, limiting the observations of their impact on human settlements. However, rheological models based on morphological and petrological datasets can contribute to decipher the eruptive dynamics and durations of ancient eruptions. The Malpaís de Zacapu, a temporal-spatial monogenetic volcano cluster at the western margin of the Zacapu lacustrine basin (Michoacán, Mexico), offers a good opportunity to apply such models because of the availability of a high-resolution LiDAR topography from which detailed morphological data was extracted. The Malpaís de Zacapu comprises late Holocene lava flow fields emplaced in the last 3200 years by four different low magnitude volcanic eruptions: Infiernillo, Malpaís Las Víboras, Capaxtiro, and Malpaís Prieto. Jointly these eruptions produced thick andesitic block lava flows covering an area of 38.3 km^2 with a volume of ~4.4 km^3. The lava viscosities at eruption vents were estimated from petro-textural analyses and range between 10^3 and 10^6 Pa s, while the final flow apparent viscosities, obtained from dimensional analyses, vary from 10^8 to 10^{10} Pa s. We estimated the mean effusion rate and lava flow emplacement duration for each flow field. Results revealed that the more viscous flows, Malpaís Las Víboras and Malpaís Prieto, could have been emplaced in less than 3 years, while the more fluid Infiernillo probably took less than 1 year. In stark contrast, the morphologically different and more voluminous Capaxtiro flow field could have been emplaced in ~27 years. These findings can help to evaluate the impact that these eruptions had on adjacent pre-Hispanic populations, known to have inhabited the region since at least 3000 years ago.

Keywords Michoacán-Guanajuato volcanic field · Viscosity · Eruption duration · Andesite · Archaeology · LiDAR · Zacapu

Introduction

Lava flows are common landforms in monogenetic volcanic fields regardless of their tectonic context. Monogenetic mafic lava flows are often related to fissure eruptions and scoria cone structures (Hawaiian- to Strombolian-type eruptions; Cas and Wright 1988; Kilburn 2010; James et al. 2012). They have been extensively observed and studied allowing to establish empirical models and to estimate emplacement parameters including, e.g., lava viscosity, eruption temperature, flow velocity, effusion rate, and eruption duration (e.g., Nichols 1939; Walker 1973; Hulme 1974; Kilburn and Lopes 1991; Pinkerton and Wilson 1994; Harris and Rowland 2009; Chevrel et al. 2013; Kilburn, 2010). In contrast, silicic monogenetic flows (andesitic to rhyolitic *coulée*-type structures) often lack a prominent vent edifice, and their formation and emplacement dynamics are not yet well-constrained due to infrequent direct observation (examples of observed active andesitic lava flows are Paricutin, Krauskopf 1948; Lonquimay, Naranjo et al. 1992; and flows at stratovolcanoes such as Colima, Navarro-Ochoa et al. 2002; Arenal, Cigolini et al. 1984; Sinabung, Carr et al. 2019). To constrain past silicic lava flow parameters, models established from mafic compositions have been employed (e.g.,

Editorial responsibility: H. Dietterich

Deputy Executive Editor: J. Tadeucci

✉ Nanci Reyes-Guzmán
nanreyguz@gmail.com

1 Departamento de Vulcanología, Instituto de Geofísica, Universidad Nacional Autónoma de México, C.P. 04510, Coyoacán, Mexico

2 CNRS, IRD, OPGC, Laboratoire Magmas et Volcans, Université Clermont Auvergne, F-63000, Clermont-Ferrand, France

3 Archéologie des Amériques, UMR 8096– CNRS and Université Paris 1, Paris, France

Latutrie et al. 2017; Chevrel et al. 2016b; Larrea et al. 2017; Ramírez-Uribe et al. 2021).

Recent studies have included the use of high-resolution light detection and ranging (LiDAR) images to better map and delimit single lava flows and their different lobes. Some have focused on active lava flows and their changes in morphology along their emplacement paths (e.g., Etna lava flow, Mazzarini et al. 2007; Favalli et al. 2010; Tarquini and de Michieli 2014). Others have established stratigraphic relationships between different lava flow units, calculated lava viscosities, effusion rates, and eruption durations by using morphological approaches (Deardorff and Cashman 2012; Tarquini et al. 2012; Deligne et al. 2016; Dietterich et al. 2018; Younger et al. 2019; Ramírez-Uribe et al. 2021).

The hazard evaluation of lava flows can be better constrained by approaching their rheological properties even though the volcano is inactive (e.g., Hulme 1974; Kilburn and Lopes 1991; Griffiths 2000; Gregg and Fink 2000; Chevrel et al. 2013; Castruccio et al. 2013). In Mexico, only few studies on the rheology of lavas have been published: Colima volcano (Lavallée et al. 2007), Citlaltépetl volcano (Carrasco-Núñez 1997), and some in the Michoacán-Guanajuato Volcanic Field (MGVF; e.g. Chevrel et al. 2016b; Larrea et al. 2017; 2019a; Ramírez-Uribe et al. 2021). However, the historic eruptions of Jorullo (1759–1774) and Paricutin (1943–1952) volcanoes were important to realize the impacts of monogenetic eruptions on small towns (Rowland et al. 2009; Fries 1953). They were both preceded by months of significant earthquake activity causing fear among nearby populations, and when the magma finally erupted, ash fallout covered extensive farmlands and forested areas and the flowing lavas forced people in nearby towns to abandon their homes and resettle elsewhere (e.g. Gadow 1930; Wilcox 1954; Nolan and Gutiérrez 1979; Guilbaud et al. 2009). With these examples arises, the question of how older eruptions might have affected ancient populations in the MGVF.

To answer this query, here we focus on the morphological features and emplacement dynamics (viscosities, eruption durations) of the Malpaís de Zacapu lava flows, a temporal-spatial monogenetic volcano cluster at the western margin of the Zacapu lacustrine basin (ZLB), situated in the Michoacán-Guanajuato Volcanic field (MGVF; Fig. 1) using a LiDAR image (Fig. 2) with a 50-cm-resolution made expressly for the MESOMOBILE-Michoacán archaeological project with the aim to better understand their impact on ancient human populations in this region. The topographic data allowed precise mapping and measurement of the different flow units and of their morphological features (vents, pressure ridges, levées, front margins, lobes, lengths, widths, and thicknesses). By combining these results with petrological work on various lava samples (whole-rock and mineral chemistry, mineral-equilibrium temperature estimates), we calculated magma and lava viscosities and inferred eruption dynamics and durations.

The Malpaís de Zacapu

The Holocene Malpaís the Zacapu cluster, located at the western margin of the Zacapu lacustrine basin (ZLB) started with the eruption of the Las Vigas scoria cone that produced the Infiernillo lava flow dated at 3200 years BP (Reyes-Guzmán et al. 2018). It is followed in chronological order by the Malpaís Las Víboras, Capaxtiro, and Malpaís Prieto lava flows (Fig. 2), which emanated from different vents (Mahgoub et al. 2018). These four volcanoes are collectively called Malpaís de Zacapu. *Malpaís* (badland in Spanish) is a term that refers to land unsuitable for agriculture, such as the rocky substrate devoid of soil that characterizes these four young lava flows (Fig. 3).

Previous studies related to the MGVF have revealed that the area was inhabited since at least 3000 years BP (date obtained on *Zea mays* pollen; Watts and Bradbury 1982), and several investigations of Holocene volcanoes have shown that eruptions in prehistoric time have been frequent, affecting human populations, as well as providing materials for construction and tool manufacture (e.g. Hasenaka and Carmichael 1985a, b, 2017b, 2018; Hasenaka 1994; Fisher 2005; Forest 2014; Chevrel et al. 2016a, b; Kshirsagar et al. 2016; Darras et al. 2017; Mahgoub et al. 2017a; Reyes-Guzmán et al. 2018; Larrea et al. 2019a, b; Ramírez-Uribe et al. 2019). According to Faugère (2006), the human occupation near the ZLB initiated between 5000 and 2000 BC in the Lerma river valley (to the N of ZLB) and around 2000 BC the ZLB became sparsely occupied. The archaeological record becomes better documented since 100 BC (e.g. Michelet 1992; Michelet et al. 1989; Arnauld et al 1993; Arnauld and Faugère-Kalfon 1998) and indicates four main phases of permanent human occupation around Zacapu lake, which are: Loma Alta (100 BC-AD 550), Lupe (AD 600–850), Palacio (AD 900–1200), and Milpillas (AD 1200–1450). Since phase Loma Alta, the swamps of the ZLB were inhabited by local people, but the occupation expanded to the NW edge of the western ZLB on the surface of Late Pleistocene lava flows (Dorison 2019). During the end of Lupe and the beginning of Palacio phases, the sites became abandoned, and a drastic population reduction occurred; the population moved to the north (Lerma valley), while the Palacio site located on the distal margin of El Capaxtiro's widest lava flow unit (Fig. 2c), concentrated a large portion of the population. During the Milpillas phase, the population increased to ~ 15,000 inhabitants (Michelet 1992; Michelet et al. 1989; 2005; Pétrequin 1994; Darras 1998) living in urban areas erected on the surfaces of the Infiernillo, Capaxtiro, and Malpaís Prieto lava flows. After 2–6 generations (AD ~ 1400/1430), this large population migrated to Pátzcuaro lake for reasons that remain poorly understood.

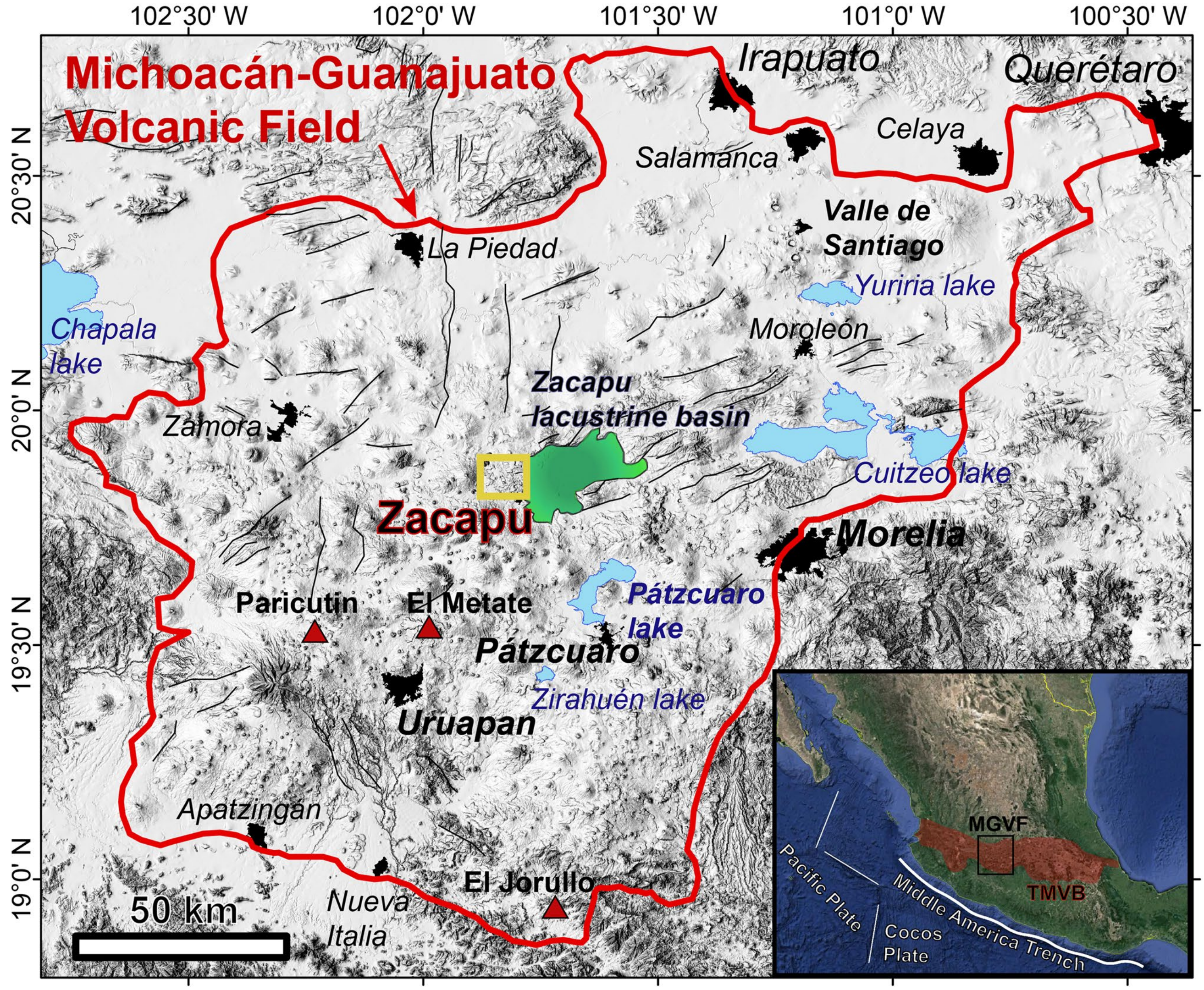

Fig. 1 Digital elevation model (taken from INEGI 2020) of the Michoacán-Guanajuato volcanic field (MGVF, outlined in red) showing lakes (in blue), the Zacapu lacustrine basin (in green), volcanoes younger than 900 years (red triangles), major faults (black lines), and cities. Yellow quadrangle indicates the study area shown in detail in Figs. 2, 4 and 5. Inset map at the lower right corner shows the location of the MGVF within the Trans-Mexican Volcanic Belt (TMVB)

This work contributes to the better understanding of volcanism in this area and its relationship with the history of human occupation, which in turn can help to reduce the impact of future eruptions in this region.

Methods

Geologic fieldwork to ground-proof landform limits and to sample lava flows were carried out and reported by Reyes-Guzmán et al. (2018). Here we used twenty-seven of the rock samples that were previously collected and chemically analyzed for major and trace element abundances at Activation Laboratories LTD (Ancaster, Canada) by fusion-inductively couple plasma (FUS-ICP), total-digestion inductively couple plasma (TD-ICP), and multi-instrumental neutron activation analysis (INAA). Modal mineralogical compositions were obtained from point counting (1000 points counted per thin section) using an automatic point counter mounted on a microscope which moves the thin section holder in controlled steps in *X*–*Y* directions. Thirteen of them were selected to determine mineral compositions using a JEOL JXA-8230 electron microprobe at the Laboratorio de Microanálisis at the Instituto de Geofísica (Campus Morelia, UNAM). Measuring conditions were set at an accelerating voltage

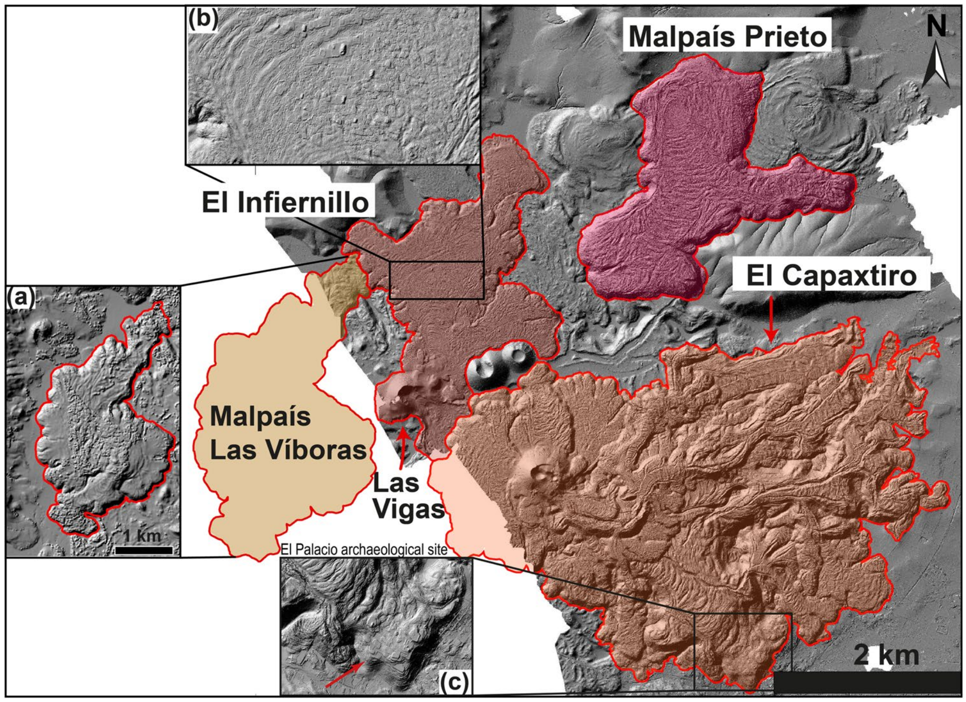

Fig. 2 Hill-shaded LiDAR-image of the Malpaís de Zacapu lava flow field. Colored polygons delimit the area covered by each of the four Late Holocene lava flows. Note that Malpaís Las Víboras is not covered by the LiDAR image but by another 5-m-resolution DEM (taken from INEGI 2020) shown in (**a**). (**b**) Image of pre-Hispanic anthropogenic modification on Infiernillo lava surface. (**c**) El Palacio archaeological site on Capaxtiro lava flow (red arrow)

of 15 kV and a beam current of 10 nA (1 to 10 μm in diameter), and counting times of 40 s for Ti, Fe, and Mg, and 10 s for K, Na, Ca, Si, and Al. Glass compositions could not be measured because of the high density of microlites in the rock matrixes.

Mineral compositions in each thin section were used to apply a suite of geothermobarometers based on the equilibria between olivine-liquid (Beattie 1993), clinopyroxene-orthopyroxene (Brey and Köhler 1990), orthopyroxene-liquid (Beattie 1993), and clinopyroxene-liquid (Putirka et al. 1996). For each geothermobarometer, the equilibrium between the phases involved was tested following the instructions in the respective studies, and non-equilibrated phases were rejected. For pre-eruptive conditions, we considered the equilibrium between the mineral and the bulk-rock composition, while for syn-eruptive conditions we considered the equilibrium between the mineral and the residual liquid composition. The residual liquid composition was estimated by subtracting the composition of each mineral phase (according to their vol.%) from the bulk-rock composition and by following the ideal fractional crystallization sequence (olivine-plagioclase-orthopyroxene-clinopyroxene; see online resource 1). To determine the olivine crystallization temperature, we assumed pressures between 800 and 500 MPa following Hasenaka and Carmichael (1987) and Hasenaka (1994). For the other minerals, crystallization pressures were obtained following the Putirka (2008) and Neave and Putirka (2017) geothermobarometers. The H_2O content at pre-eruptive conditions was obtained from the plagioclase-liquid equilibrium following the Water and Lange (2015) hygrometer, while assuming H_2O to be 0.1 wt.% for syn-eruptive conditions (following Chevrel et al. 2016b).

The viscosity of the magma (pre-eruptive) and lava (syn-eruptive) depends on the temperature, chemical composition, mineral and bubble content (and shape), and H_2O-content, which change during the eruption (e.g., Lipman et al. 1985; Lipman and Banks 1987; Moore 1987; Crisp et al. 1994; Cashman et al. 1999; Giordano et al. 2008; Muller et al. 2010; Mader et al. 2013). Here, we compute the effective viscosity of the lavas that is defined as the product of the liquid (melt) viscosity and the effect of the crystals that is defined as the relative viscosity (Eq. 1 in online resource 2). We also calculated the effect of bubbles on the viscosity by following the Phan-Thien and Pham (1997) approach. However, the viscosity was not significantly affected (only values for two samples differed by one order of magnitude, while the others remained within the same magnitude). For this reason, we did not further consider the potential effect of bubbles on viscosity in this study. The liquid viscosity was calculated following the Giordano et al. (2008) model which requires the temperature and the recalculated liquid compositions (without phenocrysts for pre-eruptive conditions, and without micro-phenocrysts for syn-eruptive conditions) including the water content depending on the pre-eruptive or syn-eruptive conditions. The relative viscosity was calculated using the equation of Maron and Pierce (1956) where the maximum packing fraction of crystals is obtained following Muller et al. (2010) and Mader et al. (2013). We considered two crystal families: the first are elongated crystals (e.g., plagioclase) with aspect ratios of 4.7, and maximum

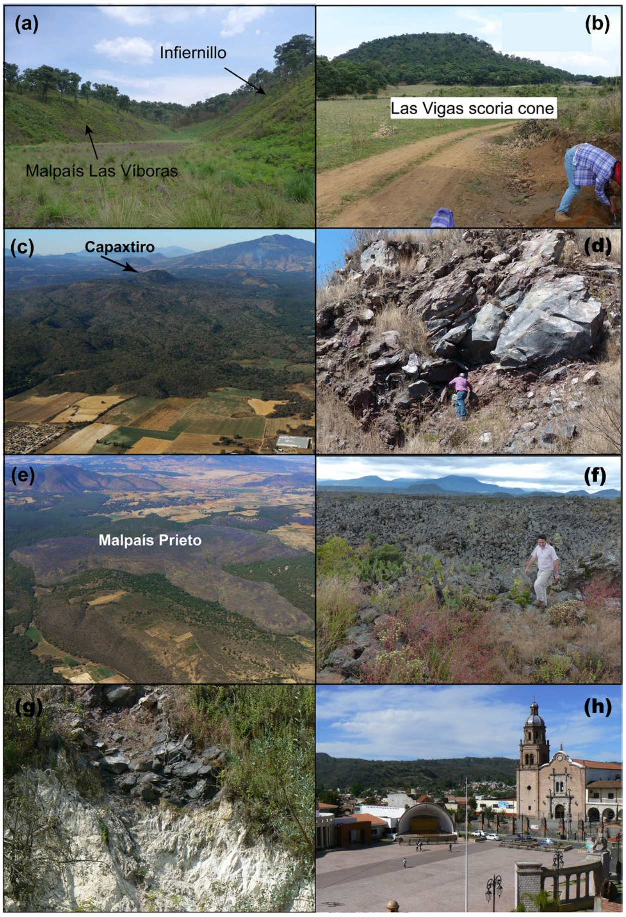

Fig. 3 Lava flow photos: (**a**) Contact between Infiernillo and Malpaís Las Víboras. (**b**) View of the Las Vigas scoria cone from ~1 km distance. (**c**) Aerial view of the Capaxtiro lava field and its main vent from the E. (**d**) Quarry displaying internal blocky structure of a Capaxtiro lava flow (located near sampling location 1018 shown in Fig. 5). (**e**) Aerial view of Malpaís Prieto lava flow from the SE. (**f**) Malpaís Prieto northern lava flow surface. (**g**) Lake deposits (~3 m) under Capaxtiro's southern lava flow. Taken from Reyes-Gumán et al. 2018. (**h**) View of Capaxtiro's distal lava flow front from Zacapu City

packing of 0.454. The second family includes spherical or equant crystals (e.g., olivine and pyroxene) with a maximum packing of 0.641 (Eqs. 2 and 3 in online resource 2). Crystallinities were normalized to exclude the pore volume.

Finally, we used a high-resolution (50 cm) LiDAR dataset from which a digital elevation model (DEM) and a hill-shade image (Fig. 2) were generated, and a DEM (5-m-resolution; Fig. 2a) built from the topographic data from the Instituto Nacional de Estadística, Geografía e Informática (INEGI) using ArcView Geographic Information System (ArcGis). We drafted the main morphological surface features of lava flows, which are difficult or impossible to identify on regular aerial photos. This allowed the unambiguous identification of vents and single lava units, and the reconstruction of their flow paths and directions. Additionally, we accurately measured the morphological parameters such as length, width, thickness, and slope of lava flows and channel widths. Between 5 and 10 cross-sections perpendicular to the flow's direction (Figs. 4 and 5) were extracted to get average values and error estimations of width and thickness. The area delimitation and the average thickness aided to estimate the volume of each lava flow conforming the Malpaís de Zacapu. Flow dimensions were then used to estimate flow velocity, effusion rate, and apparent flow viscosities (integrating the effect of the core and crust during the emplacement), as well as emplacement duration following the methodology outlined in Chevrel et al. (2016b). For this, we used the Grätz-number approach that links the final length of the flow to the amount of cooling taking place throughout the lava by conduction considering the velocity of flow emplacement (Pinkerton and Sparks 1976; Hulme and Fielder 1977; Pinkerton and Wilson 1994: see Eq. 4 in online resource 2). Flow viscosity was then estimated from the equation of Jeffreys (1925) adapted by Nichols (1939; Eq. 5 in online resource 2). The mean volumetric effusion rate of the extruded lava is then simply estimated by the product of the velocity of flow emplacement and the cross-section area of the flow (average width × average thickness; Eq. 6 in online resource 2). Flow yield-strength was estimated using the gravitational basal shear-stress equation (Hulme 1974; Wilson and Head 1983; Eq. 8 in online resource 2). Flow emplacement durations were finally estimated by dividing the total lava flow volume by the mean volumetric effusion rate (Eq. 7 in online resource 2). Alternatively, we also followed the Kilburn and Lopes (1991) method which derived an equation that relates the emplacement duration to the final dimensions of the flow, independently of the effusion rate, lava intrinsic properties (viscosity, density), and driving forces (gravity) but accounting for surface heat loss by radiation and conduction (Eq. 16 in Kilburn and Lopes (1991) or Eq. 9 in online resource 2). Errors reported in Table 2 for morphological features are standard deviations from the mean values, while for the calculated parameters (viscosity, yield-strength, effusion rate, and eruption time), errors are calculated by the propagation of uncertainties (partial deviation of each variable; see online resource 2), and a lava density of 2600 kg/m^3, as usually considered (Harris et al. 2004; Chevrel et al. 2016b).

Results

Morphology of lava flows

The Malpaís de Zacapu consists of four closely spaced monogenetic Holocene volcanoes paleomagnetically dated by Mahgoub et al. (2018) in conjunction with one ^{14}C date

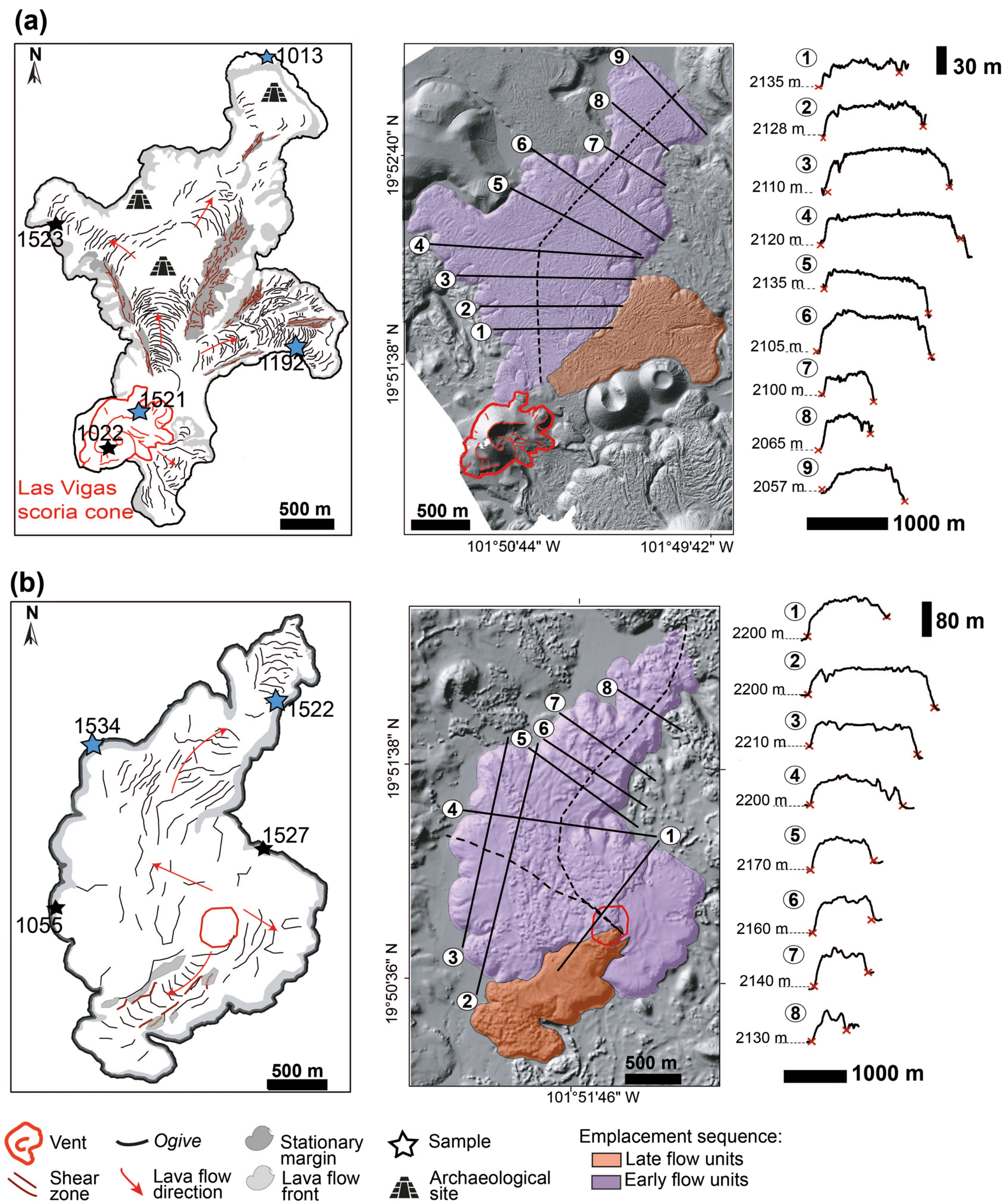

Fig. 4 Sketch map and hill-shaded DEM showing main morphological features and elevation profiles of: **(a)** Infiernillo lava flow, **(b)** Malpaís Las Víboras. Stars indicate sampling locations, in blue those used for mineralogical analyses

previously obtained by Reyes-Guzmán et al. (2018). They can be easily distinguished in the field due to their differing morphologies and stratigraphic relations (Figs. 2 and 3). The oldest two, Infiernillo and Malpaís Las Víboras, are

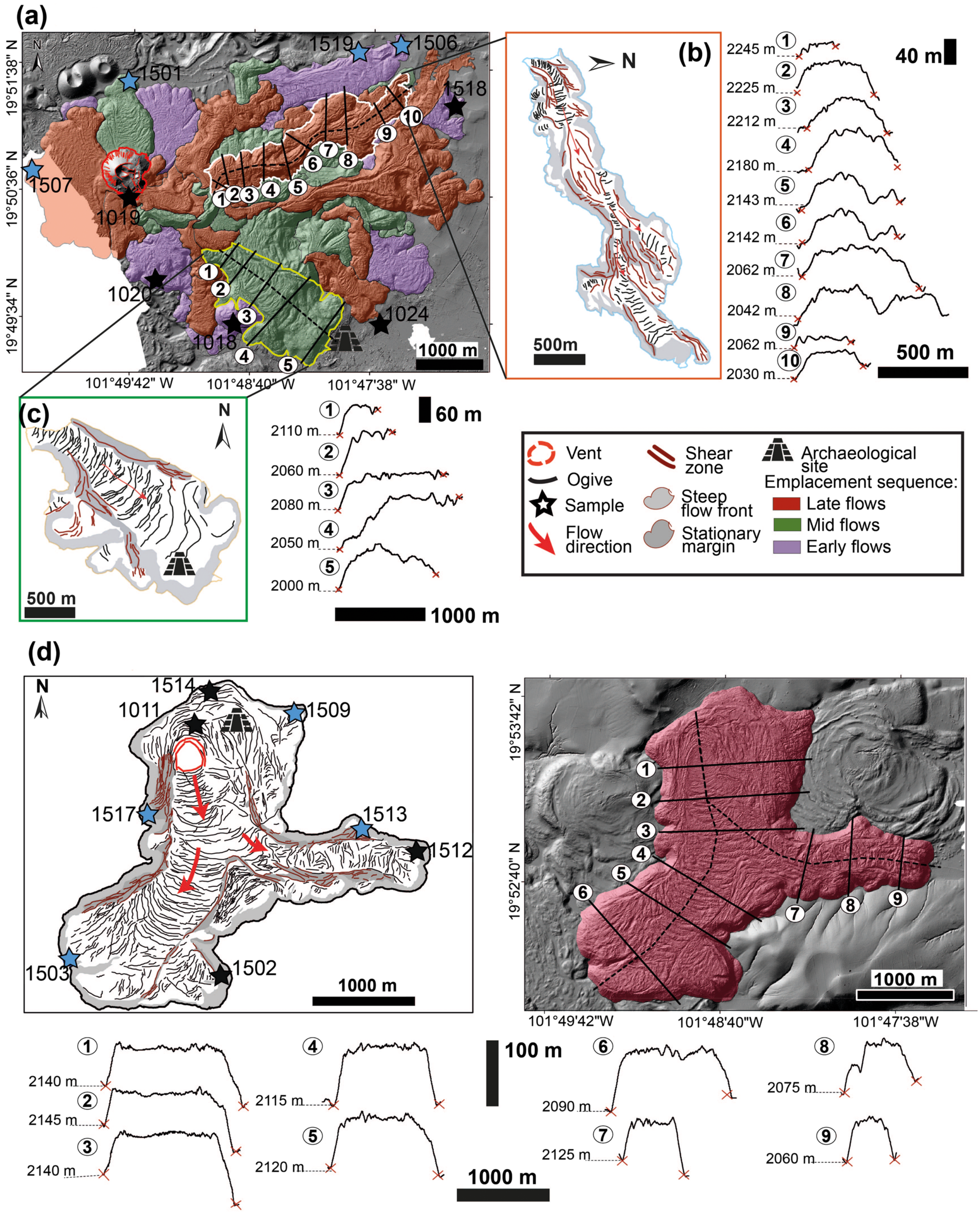

Fig. 5 (**a**) Hill-shaded DEM of Capaxtiro lava flow field indicating elevation profiles. (**b**) The longest lava unit from el Capaxtiro displaying main morphological features. (**c**) The widest lava unit from Capaxtiro displaying main morphological features. (**d**) Sketch map and hill-shaded DEM showing main morphological features and elevation profiles of Malpaís Prieto. Stars indicate sampling locations, in blue those used for mineralogical analyses

occupied by an oak forest that grows on an incipient thin soil (Fig. 3a). Capaxtiro supports some shrubs (Fig. 3c), while the youngest, Malpaís Prieto, is almost devoid of any vegetation and exhibits its barren and inhospitable dark lava (Fig. 3e, f). At a first glance of the LiDAR image (Fig. 2) and aerial photograph (Fig. 3c), we can observe that both, Infiernillo and Capaxtiro, have a prominent vent edifice (scoria cone and dome, respectively; Fig. 3b, c), while the exact sources of Malpaís Prieto and Malpaís Las Víboras are not apparent. Infiernillo, Malpaís Las Víboras, and Malpaís Prieto can be classified as a simple flow field, while Capaxtiro is a compound flow field. In the following section we describe in detail the morphology of each volcano.

Infiernillo

Chronologically, the first volcano erupted at 3200 ± 30 years BP (1490–1380 BC; Reyes-Guzmán et al. 2018), and it is formed by Las Vigas scoria cone (Fig. 3b), which displays a horseshoe-shaped crater open to the SE, and by the lava flow forming Infiernillo (Fig. 4a). This flow is divided into two distinct units. One unit flowed northward forming two main lobes, one to the N-NW and the other to the N-NE (Fig. 4a). The longest to the N-NE reached ~ 3100 m from the vent, has an average thickness of ~ 27 m, and a width ranging between 250 and 1000 m. The second flow unit flowed to the NE and is ~ 1700-m long, 500-m wide, and ~ 25-m thick. Both lava flows display marginal levees, shear zones, and cross-flow ridges (ogives). Flow fronts are steep and end with multiple 50–200 m wide toes, except the flow front to the N-NE that presents a stepped profile that was formed presumably from a basal breakout (Fig. 4a). Infiernillo flows are classified as blocky ‘a‘ā to block type due to the broken flow surface composed of a heterogeneous rubbly mixture of clinker clasts (irregular and heterogeneous rock fragments with vesicular surfaces with denser inner parts) and angular dense blocks with flat and smooth surfaces (Harris and Rowland 2015).

The first flow was noticeably modified by ancient people who adapted its surface to their needs and built a settlement by relocating loose lava blocks on its surface and using them as building material for walls, terraces, and foundations (Fig. 2b). On Fig. 4a, we drafted the ogives (perpendicular to flow direction), which are clearly absent in the artificially disrupted areas (see also Fig. 2). The total area covered by the Las Vigas cone and its exposed Infiernillo lavas encompasses 5.1 km^2 with a volume of 0.29 km^3 of magma (Reyes-Guzmán et al. 2018).

Malpaís Las Víboras

The second eruption, Malpaís Las Víboras (Fig. 4b), was dated at 1340–940 BC (Mahgoub et al. 2018). This structure is just outside the LiDAR image but integrated into a 5-m-resolution DEM (Fig. 2a). Although the morphological features (e.g., levees, shear zones) are less visible on this DEM, we can discern flow directions and different lava flow units. The vent area can be identified because the lava flow surface describes concentric ogives around a spot in the south-central area (Fig. 4b). This area is ~ 350 m in diameter and slightly higher (~ 20 m) than its surrounding terrain. The first flow unit seems to have flowed radially around the source point and elongated toward the N-NE reaching a length of ~ 2500 m, a width of ~ 1600 m, and a thickness of 100 m. It was followed by a short flow unit emplaced toward the SW that leans against an older lava flow (emitted from Las Cabras scoria cone, see Reyes-Guzmán et al. 2018). This late lava unit displays a central channel marked by ogives perpendicular to flow direction and is embraced by well-defined shear zones. The emitted lava flow is defined as block type due to the clastic surface made of large (up to 2 m), dense, slightly angular to rounded blocks with smooth surfaces. No well-defined channels are visible on the largest flow, but the SE unit shows a succession of ogives and lateral zones (Fig. 4b). Flow fronts are steep and end with wider toes than Infiernillo (100–500 m).

Capaxtiro

The third volcano, Capaxtiro, dated at 200–80 BC (Mahgoub et al. 2018) produced an extensive compound lava flow field consisting of an intricate pattern of numerous intertwined lava flows, delimited to the east by the Zacapu lake plain. In the western part of the lava field, a topographic high, intermediate in shape between a spatter cone and a dome (Fig. 3c), dominates the surrounding lava flow field. The older neighboring Infiernillo and Malpaís Las Víboras flow fields are also not covered by any ash fallout. Lava spread radially around the vent with a preferential direction eastward, reaching a maximum distance of ~ 5 km. The lava that flowed to the N and to the W formed large flat flows ending in a fan shape and multiple toes and steep well-defined fronts, while the flows to the E are a succession of imbricate narrower flows (Fig. 5a). Despite of the high-resolution LiDAR coverage, the delimitation of each flow unit was complicated. In some cases, it is not clear whether tongues are lateral breakouts or secondary lobes of a main flow. We propose that this compound flow field is composed of 28 individual lava flow units belonging to three chronological groups (early, mid, and late) based on the identification of lava front margins and lateral levees, and their stratigraphic relationships (Fig. 5a). Flow unit outlines and levees are blurred by the many breakouts and the overlying flows. At least ten units seem to have been produced from breakouts of previously emplaced flows. Breakouts are mainly either located at flow fronts or lateral levees, but at some places, the lava seems to have broken out from inflated flows through an axial large crack. Flow fronts are mainly steep, but in some places to the E, they seem to have vanished into the sedimentary deposits of the Zacapu lake. Surfaces display well-defined and deep shear zones parallel to flow direction embracing channelized lava marked by ogives perpendicular to flow direction. Some flows have narrow and sinuous channels (Fig. 5b), while others are large with a fan shape (Fig. 5c). The lava flows are made of slightly vesicular to dense angular blocks with smooth faces, typical of block lava. A small quarry at the southern margin of the flow field (near sample location 1018; Fig. 5a) reveals highly clastic fronts (Fig. 3d).

In total, the lava flow field covers an area of ~ 21 km^2 with a corresponding total erupted volume of 3.1 km^3. The average thickness of the field is 150 m but represents the sum of different overlapping lava flow units (Reyes-Guzmán et al. 2018). We measured in detail two of the best exposed lava flow units to constrain their morphological features. One of them corresponds to the longest (Fig. 5b), while the other to the widest lava flow identified (Fig. 5c). The longest flow is characterized by irregular shear zones and has two main lobes. It reached ~ 3500 m from the vent, is ~ 470-m wide, and ~ 60-m thick. In contrast, the widest flow is ~ 1000-m wide, ~ 2500-m long, and ~50-m thick. It displays a marked channel, but its levees are not well-defined, although ogives are well-preserved along most of the flow. Its steep frontal margin displays large artificial terraces separated by walls with an excellent view over the lower-lying lacustrine plain. This is the archaeological site of El Palacio, an urban area that flourished between AD 900 and AD 1200. The LiDAR image permits the identification of areas revealing significant flow surface modification (Figs. 2b, 5c) due to the displacement of lava blocks to construct terraces, houses, and temples (Pétrequin 1994; Pereira et al. 2021).

Malpaís Prieto

The fourth volcano erupted is the Malpaís Prieto, dated at AD 900 (Mahgoub et al. 2018). This is the simplest volcanic structure conforming the Malpaís de Zacapu. Its morphological features are easy to discern because its dark rocky surface has not yet developed any soil and also not been covered by vegetation (Fig. 3e, f, 5d). The Malpaís Prieto lava flow was emitted from a point source in the N with a diameter of ~ 300 m, and ~ 10 m higher than the surrounding ground, from which it flowed southward before being divided into two distinct lobes: One flowed to the E because it became diverted by an older volcano (El Pinal, Reyes-Guzmán et al. 2018), and the second continued to the S. The latter is wider and longer than the eastern lobe. Both display shear zones, static narrow levees, and large channels (up to 1-km wide) marked by concave large ogives perpendicular to flow direction. Cross-flow profiles show a flat surface and steep fronts (Fig. 5d). This flow is a block lava flow made of rubbly to blocky clasts (dm to m in scale). Malpaís Prieto is on average ~ 1400-m wide, ~ 100-m thick, and ~ 3400-m long (from its vent to the southernmost front) and covers 5.7 km^2 with a total volume of 0.5 km^3. Its northern part was also strongly modified and densely populated in pre-Hispanic time as attested by the remains of numerous terraces, walls, and pyramidal temples (Dorison 2019).

Geochemistry and petrography

Twenty-seven rock samples were chemically analyzed (whole-rock compositions are given in online resource 3), and results are plotted in the classification diagram of LeBas et al. (1986) in Fig. 6. Accordingly, most samples from all four volcanoes are calc-alkaline andesites. The samples from Infiernillo are low-silica andesite ($57 < SiO_2$ wt. % < 59) except for one bomb sample from Las Vigas cone that classifies as a trachy-basaltic andesite ($SiO_2 = 56$ wt.% and $Na_2O + K_2O = 6.2$ wt.%); in contrast, lavas from Malpaís Las Víboras and Malpaís Prieto are high-silica andesites with SiO_2 contents between 61 and 63 wt.%. Samples from Capaxtiro are slightly more silicic and reach into the dacite field with SiO_2 contents varying between 62 and 63.5 wt.% (Fig. 6).

Modal analyses of the different phases (phenocrystals, groundmass, vesicles) and mineral chemical compositions are reported in online resource 4 and 5, respectively. All collected lava samples (Fig. 7) are dense with about 6 vol.% (range 1–16 vol.%) of angular pore space, except for the two bombs collected at Las Vigas scoria cone (Infiernillo lava flow field) that contains up to 54 vol.% sub-rounded vesicles, and two rubbly samples collected near the vent of Malpaís Prieto that contain 19 to 29 vol. % of pore space. These pore spaces seem to stem from either scoriaceous surface textures or sample crystallization and contraction while cooling. In all the samples, shapes and sizes of vesicles vary widely, but the majority is elongated or irregular and < 1 mm in size while the smaller vesicles tend to be spherical. Larger vesicles seem to be the result of coalescence in the case of Infiernillo/Las Vigas samples.

Infiernillo lavas contain phenocrysts (< 11 vol.%) of olivine (< 1 mm), hypersthene (~ 0.5 mm), augite (~ 0.5 mm), and plagioclase (elongated, up to 1 mm), and occasionally hornblende with disequilibrium textures (Fig. 7a, b), which occur mainly in proximal (near-vent) areas of lava flows. Micro-phenocrysts (< 23 vol.%) consist of the same phases and sometimes form glomero-porphyritic clusters. Malpaís Las Víboras lava samples contain prismatic hypersthene and augite phenocrysts and micro-phenocrysts (4–20 vol.%), as

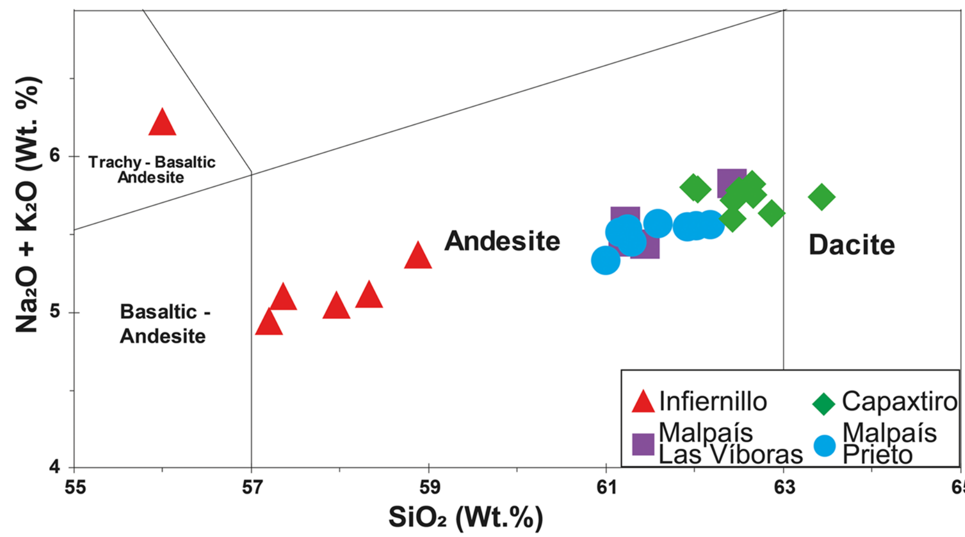

Fig. 6 Total alkalies ($Na_2O + K_2O$) vs SiO_2 diagram after LeBas et al. (1986) for all analyzed Malpaís de Zacapu rock samples

well as hornblende crystals displaying occasional opacite rims (Fig. 7c). All Capaxtiro lava samples include phenocrysts and micro-phenocrysts (< 17 vol.%) of augite, hypersthene, and plagioclase. In samples from early flows (1519 and 1506), rare olivine crystals were found, while in a sample from the late flows (1507), hornblende crystals were identified. Malpaís Prieto samples contain pyroxene and plagioclase phenocrysts (< 3 vol.%) and micro-phenocrysts (< 11 vol.%) that occasionally form clusters (Fig. 7d). Samples from the proximal area of Malpaís Prieto also contain hornblende with disequilibrium textures (Fig. 7e). All samples show plagioclase phenocrysts (< 2 mm) with sieve textures, polysynthetic twinning, and frequent disequilibrium (reabsorption) rims (Fig. 7f). Quartz xenocrysts with disequilibrium coronas of pyroxene (Fig. 7f) and occasional pseudomorphs are also encountered. Micro-phenocrysts and microlites are acicular and commonly arranged in a trachytic texture. In all samples, the groundmass is microcrystalline, and no clear glass was found, for the exception of one glassy Capaxtiro sample.

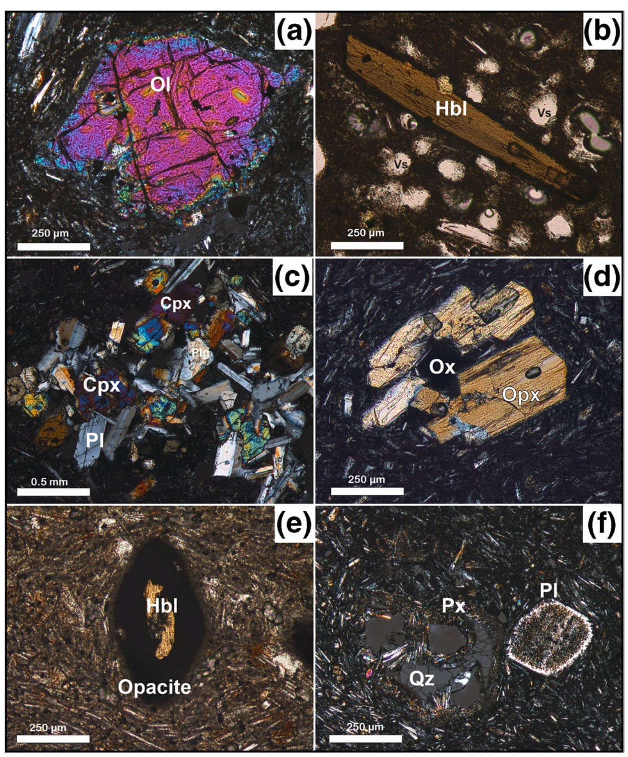

Fig. 7 Photomicrographs of Malpaís de Zacapu lava flow samples: (**a**) Olvine (Ol) phenocryst in Infiernillo. (**b**) Hornblende (Hbl) phenocryst with opacite-rim in Infiernillo bomb, vesicles (Vs) are visible. (**c**) Cluster of augite (Cpx) and plagioclase (Pl) phenocrysts in Malpaís Las Víboras. (**d**) Cluster of hypersthene (Opx) phenocrysts with an oxide (Ox) in Capaxtiro. (e) Opacite with hornblende-core embedded in a groundmass of plagioclase microlites and glass. (**f**) Quartz (Qz) xenocrystal with reaction rim of pyroxene (Px) and sieved plagioclase phenocryst in Malpaís Prieto

Thermobarometry and hygrometry

Results are depicted in Fig. 8 and listed in online resource 6. Here, we present ranges of P–T conditions. The Infiernillo magma P–T conditions ranged between 1186 ± 43 °C (distal northern lava front) and 1068 ± 38 °C at 150 ± 280 MPa for the eastern lava front. The Malpaís Las Víboras shows average P–T conditions of 1083 ± 20 °C at 0.2 and 120 ± 140 MPa by applying the clinopyroxene-liquid geothermobarometer (individual P–T calculations did not reveal significant variations) and between 1017 ± 38 °C at 240 ± 280 MPa and 977 ± 38 °C at 420 ± 280 MPa (by using the two-pyroxene geothermobarometer). Capaxtiro had a T of 1065 ± 43 °C at 500 MPa according to the olivine-liquid geothermometer, and P–T conditions ranged from 1085 ± 26 °C at 100 ± 260 MPa and 1019 ± 38 °C at 360 ± 280 MPa. For the Malpaís Prieto, P–T conditions varied between

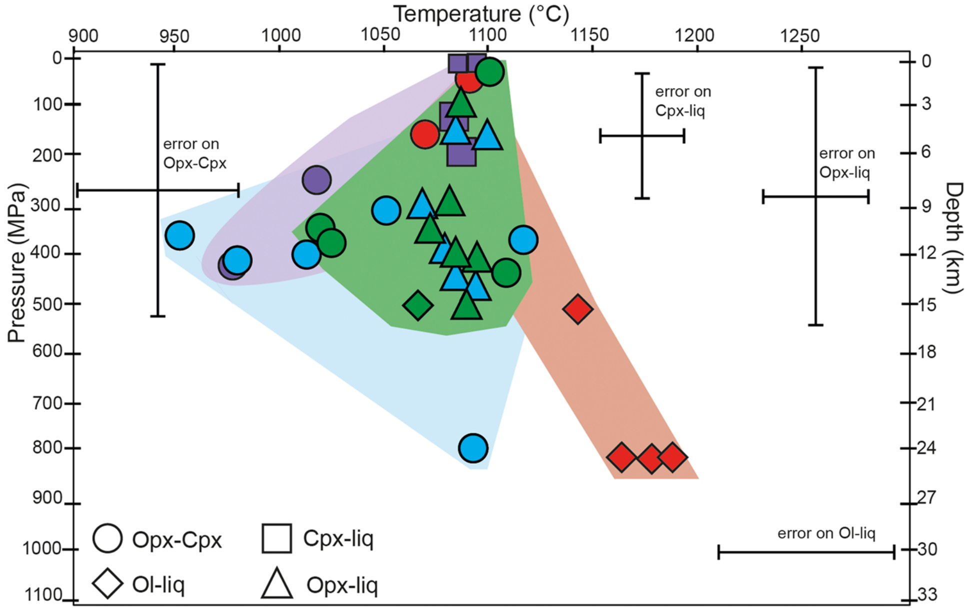

Fig. 8 Pressure–temperature diagram showing results of different mineral-equilibrium thermobarometry methods applied in this study. Data obtained by the olivine-liquid (diamond), the two-pyroxene (circle), the orthopyroxene-liquid (triangle), and the clinopyroxene-liquid (square) thermobarometers are plotted together with their respective error bars. Red, purple, green, and blue fields indicate P–T paths of Infiernillo, Malpaís Las Víboras, Capaxtiro, and Malpaís Prieto lavas, respectively

1094 ± 26 °C at 160 ± 260 MPa (western lava front) and 951 ± 38 °C at 150 ± 280 MPa (mid-lava front). Water contents ranged from 0.4 to 1.7 wt.% H_2O for Infiernillo, from 1.2 to 3.2 wt.% H_2O for Malpaís Las Víboras, from 1.3 to 2.7 wt.% H_2O for Capaxtiro, and from 1.6 to 3.4 wt.% H_2O for Malpaís Prieto.

Magma and lava rheology from petrological and morphological constraints

Calculated viscosities of the ascending magma (pre-eruptive conditions; Table 1, Fig. 9; online resource 7) vary from 3.5×10^2 Pa·s (0.4 wt.% H_2O, 4. vol.% phenocrysts, 1186 °C) to 7×10^2 Pa·s (0.6 H_2O, 5.3 vol.% phenocrysts, 1176 °C) for Infiernillo lava flows. For Malpaís Las Víboras, the magma viscosities range from 1.9×10^3 Pa·s (1.4 wt.% H_2O, 10.3 vol.% phenocrysts, 1096 °C) to 4.3×10^3 Pa·s (1.2 wt.% H_2O, 10 vol.% phenocrysts, 1082 °C). Viscosities of Capaxtiro magma vary from 7.9×10^2 Pa·s (2.3 wt.% H_2O, 2 vol.% phenocrysts, 1079 °C) to 5.3×10^3 Pa·s (1 wt.% H_2O, 6.1 vol.% phenocrysts, 1091 °C), while for Malpaís Prieto viscosities vary from 2.7×10^2 Pa·s (2.8 wt.% H_2O, 0.5 vol.% phenocrysts, 1094 °C) to 1.3×10^3 Pa·s (1.9 wt.% H_2O, 1.6 vol.% phenocrysts, 1092 °C).

Table 1 Magma and lava viscosities estimated from petrological data

Pre-eruptive conditions							Syn-eruptive conditions			
							0.1 wt% H2O			
Sample no	Volcano	H_2O [wt.%]	T [°C]	η_{liq} [Pa*s]	η_r [Pa*s]	η_{app} [Pa*s]	T [°C]	η_{liq} [Pa*s]	η_r [Pa*s]	η_{app} [Pa*s]
1013	Infiernillo	0.40	1186.0	2.8×10^2	1.23	3.4×10^2	1090.5	9.3×10^3	5.09	4.7×10^4
1192	Infiernillo	0.60	1176.5	5.6×10^2	1.25	7×10^2	1068.7	7.4×10^4	3.74	2.7×10^5
1534	Las Víboras	1.38	1096.0	1×10^3	1.80	1.8×10^3	977.0	5.5×10^5	3.38	1.8×10^6
1522	Las Víboras	1.19	1082.7	2.4×10^3	1.76	4.3×10^3	1086.6	6×10^4	8.18	4.9×10^5
1503	Malpaís Prieto	2.82	1094.5	2.7×10^2	1.02	2.7×10^2	1012.0	2.4×10^5	1.75	4.2×10^5
1513	Malpaís Prieto	2.34	1084.4	5.2×10^2	1.04	5.4×10^2	1067.4	7×10^4	1.32	9.3×10^4
1509	Malpaís Prieto	1.96	1092.0	1.1×10^3	1.12	1.3×10^3	979.1	9.7×10^5	1.51	1.4×10^6
1501	Capaxtiro	2.25	1079.5	7.2×10^2	1.10	7.9×10^2	1017.5	3.4×10^5	2.91	1×10^6
1519	Capaxtiro	1.67	1085.5	1.3×10^3	1.13	1.4×10^3	1080.5	6.7×10^4	2.38	1.6×10^5
1506	Capaxtiro	1.58	1089.5	1.4×10^3	1.21	1.8×10^3	1065.0	1.4×10^5	2.48	3.5×10^5
1507	Capaxtiro	1.09	1091.1	3.9×10^3	1.33	5.3×10^3	1071.4	1.2×10^5	2.68	3.2×10^5

ηr relative viscosity, *ηliq* melt viscosity, *ηapp* apparent viscosity (ηr × ηliq)

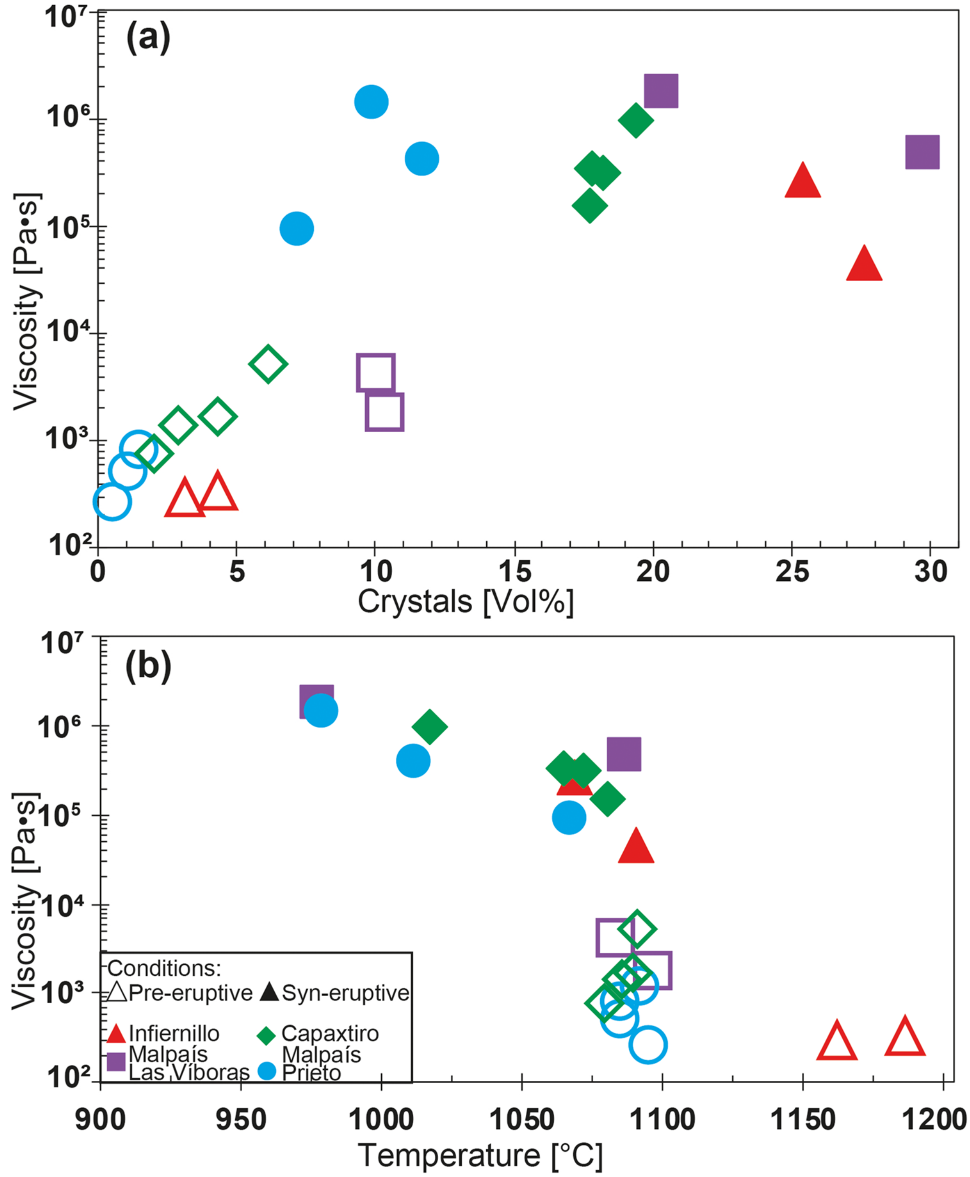

Fig. 9 Results of viscosity estimates obtained from sample petro-textural analyses. (**a**) Viscosity versus vol.% of crystals. (**b**) Viscosity versus temperature. Empty symbols indicate pre-eruptive conditions and filled symbols indicate syn-eruptive conditions. "Crystal" refers to phenocrysts at pre-eruptive conditions, and the sum of micro-phenocrysts and phenocrysts for syn-eruptive conditions

At syn-eruptive conditions (Table 1, Fig. 9; online resource 7), lava viscosities vary from 4.7×10^4 Pa·s (27.6 vol.% crystals, 1090 °C) to 2.7×10^5 Pa·s (25.3 vol.% crystals, 1068 °C) for Infiernillo, and from 4.9×10^5 Pa·s (30 vol.% crystals, 1086 °C) to 1.8×10^6 Pa·s (20. vol.% crystals, 977 °C) for Malpaís Las Víboras. For Capaxtiro, lava viscosities vary from 1.6×10^5 Pa·s (17.6 vol.% crystals, 1080 °C) to 1.0×10^6 Pa·s (20.3 vol.% crystals, 1017 °C), while for Malpaís Prieto, they vary from 9.3×10^4 Pa·s (7.2 vol.% crystals, 1067 °C) to 1.4×10^6 Pa·s (9.9 vol.% crystals, 979 °C). These results are minimum values because we did not consider the amounts of microlites, which were difficult to estimate because of the microcrystalline matrixes.

The flow velocity estimations using the Grätz-number approach (Eq. 4 online resource 2) are 47 ± 8 m/day for Infiernillo, 3 ± 0.7 m/day for Malpaís Las Víboras, 12 ± 1 m/day for Capaxtiro, and 4 ± 0.4 m/day for Malpaís Prieto. Considering the average width and thickness of each lava lobe or flow unit, these values convert to effusion rates of 14.2 ± 5 m^3/s for Infiernillo, 5.5 ± 2 m^3/s for Malpaís Las Víboras, 3.7 ± 0.7 m^3/s for Capaxtiro, and 6.2 ± 0.8 m^3/s for Malpaís Prieto. Now, using Jeffreys' equation (Eq. 5, online resource 6), we obtain a flow bulk-viscosity of 3.6×10^8 Pa·s for Infiernillo's northern lava flow (Fig. 4a), of 1.1×10^{11} Pa·s for Malpaís Las Víboras (Fig. 4b), 1.4×10^{10} Pa·s for Capaxtiro's longest lava flow (Fig. 5c), and 5.1×10^{10} Pa·s for Malpaís Prieto (Fig. 5e), with 28% to 53% of uncertainty (see Table 2). Finally, the lava flow yield strength (or basal shear-stress) calculated (Eq. 5, online resource 2) for each lava flow is 2.2×10^4 Pa, 1.1×10^5 Pa, 1×10^5 Pa, and 7×10^4 Pa, respectively, with uncertainties ranging from 11 to 14% (Table 2).

In regard to the duration of flow unit emplacements, by applying the Grätz-number approach, we obtained 67 ± 36 days for Infiernillo (northern flow), 916 ± 73 days for Malpaís Las Víboras (late lava flow), 298 ± 86 days for Capaxtiro (longest lava flow), and 862 ± 163 days for Malpaís Prieto (southern lava lobe). Finally, by applying the Kilburn and Lopes (1991) model, we obtained similar values for Infiernillo and Capaxtiro (66 ± 27 days and 291 ± 58 days, respectively), but longer times for Malpaís Las Víboras and Malpaís Prieto (2590 ± 1113 days and 345 ± 55 days, respectively, Table 2). The corresponding effusion rates of 14.4 ± 9 m^3/s and 3.7 ± 1 m^3/s for Infiernillo and Capaxtiro, respectively, are similar to those calculated by the Grätz approach, but smaller for Malpaís Las Víboras and Malpaís Prieto (2 ± 1 m^3/s and 5.2 ± 1 m^3/s, respectively).

Accordingly, using the effusion rate obtained by the Grätz approach, the Infiernillo took 0.6 ± 0.2 years (= 219 days), Malpaís Las Víboras 2.9 ± 1.4 years, Capaxtiro

Table 2 Morphological parameters, viscosities, yield strengths, and emplacement durations of the Malpaís de Zacapu lava flows

Physical constant				
Density (kg/m^3)	2600 ± 100			
Gravitational accelaration g [m/s^2]	9.81			
Grätz number Gz [-]	300			
Thermal diffusivity k [m^2/s]	4.21×10^{-7} (from Kilburn and Lopes 1991)			
Volcano	Infiernillo	Las Víboras	Capaxtiro	Malpaís Prieto
Average dimension of the flows				
Length [m]	3111 ± 34	2587 ± 136	3478 ± 28	3422 ± 87
Flow width [m]	978 ± 104	1681 ± 96	476 ± 14	1401 ± 16
Channel width [m]	509 ± 54		192 ± 15	781 ± 8
Thickness [m]	27 ± 5	100 ± 9	57 ± 3	97 ± 3
Slope [°]	1.8 ± 0.05	2.5 ± 0.2	4.1 ± 0.1	1.7 ± 0.1
Total area [m^2]	5.16×10^6	5.9×10^6	2.1×10^7	5.6×10^6
Lava flow unit volume (length*width*thickness) [m^3]	8.2×10^7	4.3×10^8	9.4×10^7	4.6×10^8
error	$\pm 1.6 \times 10^7$	$\pm 8.6 \times 10^7$	$\pm 8.5 \times 10^6$	$\pm 3 \times 10^7$
Total volume (area*thickness) [m3]	2.9×10^8	4.7×10^8	3.1×10^9	5.1×10^8
error	$\pm 1.5 \times 10^7$	$\pm 4.5 \times 10^7$	$\pm 4.1 \times 10^8$	$\pm 1.5 \times 10^7$
Aspect ratio (A/H)*	33.2	54.8	15.3	29.9
Rheological parameters from the Gz approach				
Apparent viscosity from Jeffreys´s equation [Pa × s]	3.6×10^8	1.1×10^{11}	1.4×10^{10}	5.1×10^{10}
% error	39%	53%	28%	21%
Yield strength [Pa]	2.2×10^4	1.1×10^5	1×10^5	7.1×10^4
% error	14%	21%	11%	13%
Effusion rate [m^3/s]	14.2	5.5	3.7	6.2
% error	35%	38%	20%	13%
Velocity [m/day]	46.6	2.8	11.7	4.0
% error	17%	23%	11%	9%
t_{Gz} [days]	66.8	916.4	297.7	862.2
% error	55%	8%	29%	19%
Kilburn and Lopes (1991) approach				
t_{KL} [days]	65.9	2590.0	291.3	344.9
% error	41%	43%	20%	16%
Effusion rate [m^3/s]	14.4	1.9	3.7	5.2
% error	60%	63%	29%	23%
Duration of entire eruption (V_t/Q) [years]°				
Grätz approach	0.6 ± 0.2	2.9 ± 1.4	27.1 ± 9	2.5 ± 0.4
Kilburn and Lopes approach	0.6 ± 0.4	8.2 ± 5.8	27.1 ± 11	3.1 ± 0.8

°The duration of the entire eruption considers the total volume erupted by a volcano (sum of all single lava flows or lobes indicated in Fig. 4.) and effusion rates obtained by the Grätz number and Kilburn and Lopes (1991) approaches

*Following Walker (1973), A is the diameter of the corresponding circle of the flow area and H is the thickness of the flow

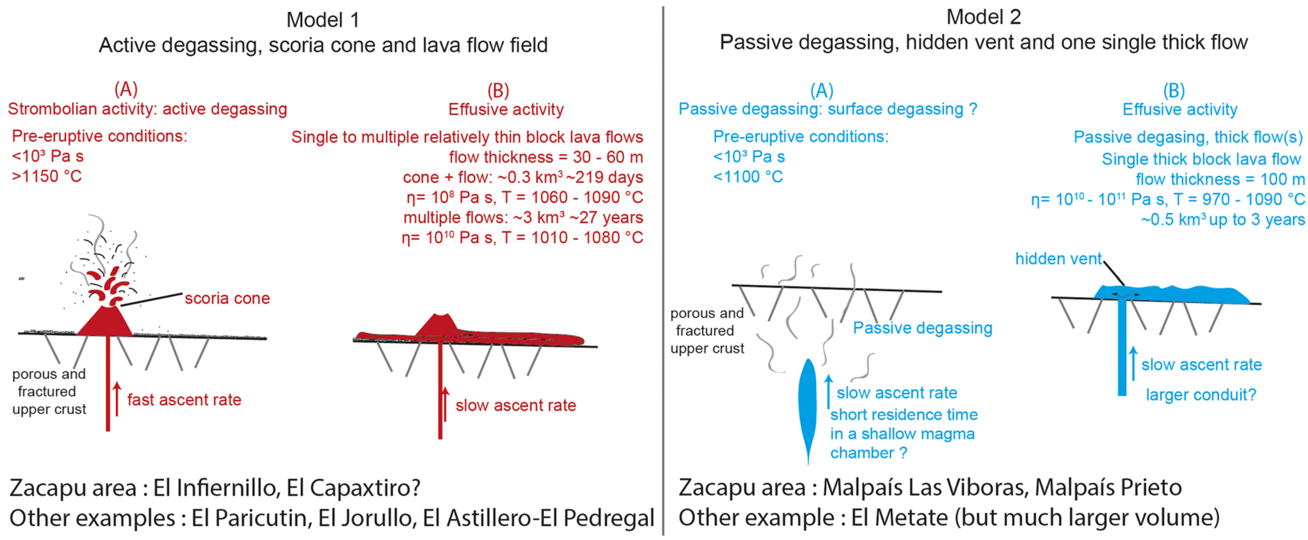

Fig. 10 Schematic eruption model for the Malpaís de Zacapu monogenetic volcanoes. Model 1 for El Infiernillo and Capaxtiro, model 2 for Malpaís Las Víboras and Malpaís Prieto. Temporal sequence of eruptive phases, magma degassing (A), and final products (B) are depicted

27.1 ± 9 years, and Malpaís Prieto 2.5 ± 0.4 years. Finally, by applying the effusion rate obtained by the Kilburn and Lopes (1991) method, we obtain 0.6 ± 0.4 years for Infiernillo, 8.2 ± 5.8 years for Malpaís Las Víboras, 27.1 ± 11 years for Capaxtiro, and 3.1 ± 0.1 years for Malpaís Prieto (Fig. 11). Note that our model assumes a constant effusion rate in which the flows were erupted in chronological sequence, one after the other (not simultaneously), without any interruptions. While this does not affect the simple flow fields (Infiernillo, Las Víboras, and Malpaís Prieto), it may underestimate the duration for Capaxtiro, if pauses in activity between flows occurred or overestimate it, if individual lobes erupted simultaneously.

Discussion

Eruption dynamics

Although the chemical composition of the Malpaís de Zacapu lava flows ranges between basaltic andesite (Infiernillo) and dacite (Capaxtiro), the largest part of the erupted volume is andesitic. Petrographically, the four volcanoes

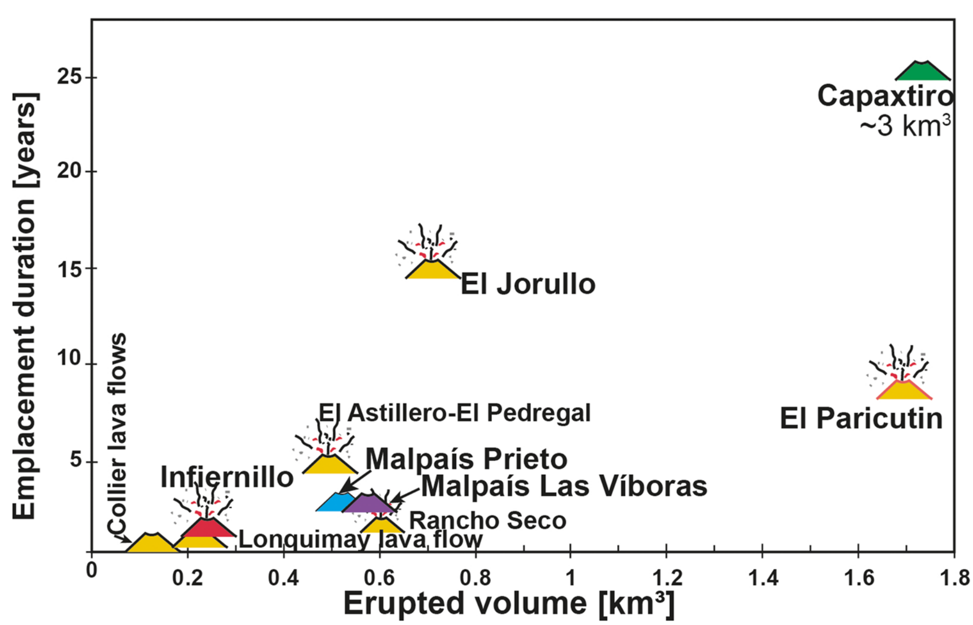

Fig. 11 Emplacement duration (years) vs. total erupted volume (km^3) diagram for all Malpaís de Zacapu volcanoes. Data for Jorullo (Rowland et al. 2009) and Paricutin (Larrea et al. 2017) historical monogenetic eruptions, El Astillero-El Pedregal (from Larrea et al. 2019a, b), and Rancho Seco (from Ramírez-Uribe et al. 2021) in the MGVF, as well as Collier (Deardorff and Cashman 2012) and Lonquimay lava flows (Naranjo et al. 1992) are shown for comparison

share similar main mineral assemblages (Opx-Cpx-Pl), but the additional presence of olivine and/or hornblende is the main distinguishing feature. Infiernillo includes both of these additional phases, while Malpaís Prieto only contains hornblende, and Malpaís Las Víboras and Capaxtiro show less than 0.1 vol.% or none of them and rarely opacite ghosts (oxides replacing the hornblende). The latter might have resulted from almost total disequilibrium breakdown of former hornblende phenocrysts during final ascent to the surface (Carmichael 2002).

The calculated temperatures and pressures (Fig. 8) indicate that pre-eruptive conditions varied and that ascent paths were complex with periods of stagnation. Pressures obtained by the orthopyroxene-geobarometer suggest temporary magma storage at 15-km depth, where orthopyroxene could crystallize. Thereafter, at 7–10-km depth, a second period of stagnation allowed clinopyroxene to crystallize, and hornblende remained barely stable. Hence, we can assume that the final ascent velocities of magma in dikes, presumably along ENE-WSW oriented normal faults, were different for each volcano.

In the following, we present a description of the eruption dynamics and provide conceptual models for the formation of the four different volcanic structures comprising the Malpaís de Zacapu (Fig. 10).

As reported in Reyes-Guzmán et al. (2018), the Malpaís de Zacapu cluster initiated with the eruption of Las Vigas scoria cone and its associated Infiernillo lava flows. This eruption started in a Strombolian fashion and with the eruption of gas-rich basaltic andesite magma (35–54 vol.% vesicles) and an olivine-plagioclase mineral assemblage in scoria-bomb samples that constitute the Las Vigas scoria cone and its associated ash fallout layers. Its horseshoe-shaped crater seems to have originated as a consequence of lateral flank collapse, likely toward the end of the eruption. The resulting deposit (either a debris avalanche or a lava flow that rafted away the missing flank of the cone on its top) could not be studied because it is largely buried under the younger lava flows produced much later by the Capaxtiro volcano (Fig. 2). After the initial explosive phase, the eruption turned effusive emplacing the Infiernillo lava flows (Fig. 10, model 1), whose final pulse emitted lavas with hornblende that partly broke down into opacite.

About 400 years after the first eruption, the Malpaís Las Víboras formed (Mahgoub et al. 2018). This volcano does not display any evidence for an initial Strombolian phase, which means that the effusive eruption of the lava flows must have occurred after degassing had taken place along the ascent path in the upper crust prior to eruption (e.g., Cas and Wright 1988). The magma probably ascended at a relatively slow rate with periods of stagnation to allow for degassing into the adjacent basement rocks (Fig. 10, model 2). The morphological steps between the lateral margins of the first and the second lava units suggest that the second was formed after the emplacement of the first unit (Fig. 4b). However, there is no evidence for an interruption of lava extrusion. In other words, both units were a product of the same pulse. The Malpaís Las Víboras samples are andesitic and show little chemical evolution (Fig. 6).

Approximately 800 years after the Malpaís Las Víboras eruption, the Capaxtiro lava flow field is emplaced (Mahgoub et al. 2018) almost purely effusively; the shape of its cone (Fig. 3c) suggests that the eruption started with an initial Strombolian phase, but ash-fallout deposits are entirely absent around Capaxtiro. Additionally, the materials forming the cone are mainly coarse dense bombs (Fig. 3d), which leads us to believe that this eruption was largely effusive in nature and may have had an explosive phase but with a low degree of fragmentation. Unfortunately, we were not able to sample systematically all of the 28 identified lava flow units (total volume = 3.1 km^3), but the occasional presence of olivine in few samples suggests differentiation from a basaltic magma, as observed at the Paricutin and Metate volcanoes (Larrea et al. 2017; 2021; Albert et al. 2020; Chevrel et al. 2016b). Additionally, the effusive eruption was accompanied by a shallow intrusion as described in Reyes-Guzmán et al. (2018). The low vesicularity of the bombs forming the small conical dome suggests that the main degassing phase occurred during slow ascent and a storage period near the surface (Gonnermann and Manga 2012). However, the gas content of this magma was seemingly at times somewhat higher in comparison to Malpaís Las Víboras and Malpaís Prieto, since at least some of it fragmented in a “mild” Strombolian fashion upon arrival to the surface producing coarse, relatively dense bombs (Fig. 10, transitional between model 1 and 2; James et al. 2012). In other words, again, the degassing occurred mostly during ascent (pre-eruptive conditions) and less during the emission and emplacement of the lava flows (syn-eruptive conditions).

Finally, ~ 1000 years after the eruption of Capaxtiro, the Malpaís Prieto erupted. Its effusive eruption style and volume (~ 0.5 km^3) is similar to that of Malpaís Las Víboras (Fig. 10, model 2), the main difference being that Malpaís Prieto shows a more pronounced chemical evolution between proximal and distal samples. The distal flows are less evolved and display a pyroxene-plagioclase mineral assemblage, while proximal samples are more silicic with a pyroxene-plagioclase-hornblende mineral assemblage. Hornblende was found only in the late products and typically shows an opacite disequilibrium rim produced during ascent, when magma was degassing (Carmichael 2002). In all four volcanoes, we found rare quartz xenocrysts with pyroxene reaction coronas and pseudomorph textures, which we interpret to have resulted from minor assimilation of shallow local basement rocks (possibly granodiorites as pointed out by Wilcox 1954; Guilbaud et al. 2009; 2011, 2012, 2019).

Dynamics and duration of lava flow emplacement

Viscosity and uncertainties

We estimated magma and lava rheological parameters from petrological analyses considering rock chemical compositions (including volatile content) and phenocryst and/or micro-phenocryst contents, but neglecting the microcrystalline matrix. This implies that we did not consider cooling and crystallization during flow. Meanwhile, the rheological parameters obtained from flow morphology (considering variables such as lava flow width, thickness, length, and slope) are based on the flow's state when it stopped, that is, when it reached rheological cut-off conditions (Chevrel et al. 2013; Kolzenburg et al. 2018). Combining these two approaches provides a range of rheological parameters during emplacement.

At Malpaís de Zacapu, lava viscosities at vent conditions range between 10^3 and 10^6 Pa·s (Fig. 2), and the final apparent flow viscosities range between 10^8 and 10^{11} Pa·s, within a range of 21 to 53% of uncertainty (Table 2). The lowest viscosity values obtained correspond to the Infiernillo flows and are related to their relatively more mafic compositions, higher eruption temperatures, as well as thinner flows in comparison to the other volcanoes (Fig. 9). The highest viscosity values correspond to the Malpaís Las Víboras and Malpaís Prieto lava flows, which, although not the most silicic, had the lowest temperatures and also higher flow thicknesses (~ 100 m, compared to 27 and 57 m for Infiernillo and Capaxtiro, respectively). The apparent flow viscosities are within the range of other andesitic block flows, like, for example, 10^9–10^{11} Pa s for El Metate lavas (up to 40% of uncertainty; Chevrel et al. 2016b), 10^8–10^9 Pa s for Rancho Seco lava flows (Ramírez-Uribe et al. 2021), 10^9–10^{10} Pa s for Colima lavas (Navarro-Ochoa et al. 2002), and 10^5–10^9 Pa s for the Lonquimay flow (Naranjo et al. 1992), but more viscous than for Paricutin (10^4–10^5 Pa s; Larrea et al. 2017). Yield strengths of all the lava flows range between 10^4 and 10^5 Pa (11 to 21% error), and are similar to those reported for El Metate (10^4 to 10^5 Pa, with 9 to 13% error; Chevrel et al. 2016b), and reflect upon lava flow thicknesses (27 to 100 m), the lowest corresponding to Infiernillo and the highest to Malpaís Las Víboras and Malpaís Prieto lava flows.

Regarding the uncertainties, it has been noticed before that changes along the lava flow morphology increase the error when applying the morphological approach (e.g Kilburn and Lopes 1991; Chevrel et al. 2013; Kolzenburg et al. 2018). In this study, the flows with the lowest uncertainties are Malpaís Prieto and Capaxtiro's longest flow (Fig. 5b), which are also the simplest flows. The highest uncertainties correspond to Malpaís Las Víboras and Infiernillo (Table 2), whose width, length, and thickness vary strongly along the flow path, increasing the error. Hence, uncertainties are larger in less constrained flows, such as Malpaís Las Víboras and Infiernillo, but lower in well-defined flows such as Malpaís Prieto.

Construction of the lava flow fields

An effusive eruption produces a flow field that may be made up of individual flow units (Guest et al. 1987; Harris and Rowland 2009). Malpaís Prieto is a single lava flow unit that was emplaced during one effusion, while Infiernillo and Malpaís Las Víboras flow fields are made of various flow units. These can be characterized by what Kilburn and Lopes (1991) termed multiple widening-type lava flow fields that widened as new flows propagated from the upstream flank of the initial flow. The Capaxtiro lava flow field is different from the others and classifies as a compound flow field due to its widening as well as superposition of discrete flows, and multiple flow breaches and overflows. Composition, temperature, and viscosity of Capaxtiro lavas do not differ significantly from the other flow fields forming the Malpaís de Zacapu, and the question rises of why the Capaxtiro flow field is so different and made of multiple intricate flow units and not of a simple or less complex flow field?

The growth of a flow field can be controlled by the interaction between the lava's hot interior (core) and the chilled outer carapace (Kilburn and Lopes 1991) and/or the balance between effusion rate and cooling rate (or viscosity increase rate; Griffiths and Fink 1992). The formation of new flows may be due to a pulsating effusion or to the cooling of the initial flows that prohibits further thickening or lengthening but triggers breakouts through the cold brittle flow carapace (e.g.Pinkerton and Sparks 1976; Krauskopf 1948; Guest et al. 1987; Pinkerton and Wilson 1994). In the case of Capaxtiro, an explanation for its particular morphology may be the following: When the early flows of Capaxtiro were emitted, they flowed preferentially to the E because to the W the Infiernillo, Malpaís Las Víboras, and Las Cabras volcanoes represented a topographic obstacle. When the lavas flowing to the E reached the lower-lying lacustrine flat, cooling must have been strong enough (maybe due to the water-soaked soft sediment) to stop them. This, together with the brake in slope, limited further flow lengthening and hindered the flow from advancing further. But lava emission continued triggering the overlaying of new flows (mid-flows; Fig. 5a), increasing the general flow field thickness (maybe similarly to the inflation process described by Kolzenburg et al. 2018). As effusion continued, the blockages generated by cooling allowed the formation of breakout lava flows that eventually formed accidentally breached flows (Pinkerton and Wilson 1994) which conformed the late lava flow unit (Fig. 5a). In other words, as the eruption continued, lava flows accumulated changing the topography which contributed to more flow bifurcations, blockages, inflations, and breakouts. Also, it might be possible that the shallow laccolithic intrusion that uplifted the lake shore at Capaxtiro's southern margin (Reyes-Guzmán et al. 2018; Fig. 3g) changed the topography aiding to the superposition of new lava flows. Without the high volume and the change in topography along the eruption, Capaxtiro would have formed a single flow or a few simple flows and become a larger version of Infiernillo (Capaxtiro's volume is ten times that of Infiernillo). Note that the Capaxtiro lavas that flowed to the W are similar in morphology to the Infiernillo flows, with similar lava flow fronts (Fig. 3h).

Comparison of emplacement rate and duration with analogue eruptions

The calculated effusion rates range between 3 and 14 m^3/s, with errors of up to 38% for the Grätz approach, and 60% for the Kilburn and Lopes (1991) approach (Table 2). Compared to the Paricutin (2–14 m^3/s; Larrea et al. 2017), Rancho Seco (4–15 m^3/s; Ramírez-Uribe et al. 2021), Collier (14–18 m^3/s; Deardorff and Cashman 2012), and Lonquimay (10–80 m^3/s; Naranjo et al. 1992) lava flows, Malpaís de Zacapu effusion rates display similar values.

The resulting emplacement duration calculated for the total volume emitted by each volcano are minimum values (Table 2). The Capaxtiro erupted ~ 3.5 km^3 (Reyes-Guzmán et al. 2018) during ~ 27 ± 10 years with an estimated effusion rate of 3.7 ± 0.7 m^3/s. This means, Capaxtiro took thrice as much time to emplace twice the volume of Paricutin (~ 1.7 km^3 in 9 years, 5.9 m^3/s mean effusion rate; Larrea et al. 2017). Capaxtiro's lower effusion rate might be related to its higher viscosity (overall higher SiO_2 content and crystallinity) than Paricutin (Larrea et al. 2017). The eruption of Infiernillo is similar in composition (olivine-bearing basaltic andesite), but smaller in volume (~ 0.3 km^3), to the Jorullo eruption (0.71 km^3 total DRE volume in 15 years; Rowland et al. 2009), hence its duration of ~ 220 ± 109 days is lower and its effusion rate of 14 ± 7 m^3/s is higher.

In the MGVF, purely effusive eruptions have not occurred in historical times, but a few studies have constrained eruption durations by a similar approach (Fig. 11): the voluminous andesitic shield El Metate emitted ~ 10 km^3 in at least 35 years (Chevrel et al. 2016b), El Astillero-El Pedregal scoria cone and associated lava flows erupted ~ 0.5 km^3 DRE of basaltic andesite to andesite magma in < 5 years, with a mean effusion rate of ~ 3.2 m^3/s (Larrea et al. 2019b), and Rancho Seco produced ~ 0.64 km^3 of andesitic magma in at least 2 years (Ramírez-Uribe et al. 2021).

In terms of chemical composition, temperature, modal mineralogy, and morphological parameters, Infiernillo lava flows may be compared to the calc-alkaline lava flows emitted by the Collier cone in Oregon (Deardorff and Cashman 2012), and the andesitic Lonquimay flow in Chile (Naranjo et al. 1992). These eruptions took 9 and 11 months to emplace 0.17 km^3 and 0.23 km^3 of magma with an effusion rate ranging between 14–50 and 10–80 m^3/s, respectively. This is comparable to our findings for Infiernillo (7–8 months to emplace 0.08 km^3 at a rate of 14 m^3/s). For Malpaís Las Víboras (volume ~ 0.5 km^3, effusion rate = 5.5 ± 2 m^3/s) and Malpaís Prieto (volume ~ 0.5 km^3, effusion rate = 6.2 ± 0.8 m^3/s), the greater volume emitted at lower effusion rates implied longer emplacement times (Fig. 11).

Implications for archaeology and future hazard evaluations

The present work adds new information on the dynamics of the Malpaís de Zacapu eruptions, allowing to better understand how volcanism could have affected ancient populations. The impact of these eruptions included the loss of farmland and disruption of daily activities. The relatively long durations of the eruptions (years to decades) accompanied by rumbling noises and seismic tremor would have inspired fear to keep people away from the proximity of the eruption sites. The forced displacement of people in nearby settlements implies a drastic change of lifestyle and relocation as observed during the eruption of Paricutin and Jorullo volcanoes (e.g., Gadow 1930; Wilcox 1954; Nolan and Gutiérrez 1979; Guilbaud et al. 2009). Since the Malpaís de Zacapu eruptions occurred in prehistoric time, eyewitness accounts in documents describing the course of events are not available. Hence, evidence for their impact on ancient populations must be sought by other means. The well-known archaeological record in the ZLB indicates that one abandonment of the basin area occurred at the end of the Lupe phase (AD 600–850; Michelet 1992; Michelet et al. 1989; Arnauld et al 1993; Arnauld and Faugère-Kalfon 1998), when Malpaís Prieto erupted (~ AD 900; Mahgoub et al. 2018). It seems that precursors of the eruption alerted the population causing fear and partial abandonment. Once the eruption initiated, almost complete relocation followed. The reoccupation of the region 300 years later (~ AD 1200) roughly coincides with a period of abandonment of the southern Lerma Basin, which had been intensively occupied during the early post-classic. A large part of the population that reoccupied the Malpaís came from that area (Arnauld and Faugère-Kalfon 1998). It is interesting to note that the Milpillas phase occupation also coincides with the timing of the eruption of the El Metate shield volcano (~ AD 1250), located 50 km SW of Zacapu, which could have caused a migration of people toward other areas, including Zacapu lake (Chevrel et al. 2016a, b). Recent archaeological studies (e.g., Forest 2014; Forest et al. 2019; Pereira et al. 2021) have revealed that the *Uacúsechas* (people that occupied the Malpaís de Zacapu) were well-adapted to dwell on the apparently inhospitable rocky substrate devoid of soil and vegetation of the lava surfaces, but also able to take advantage of nearby glassy dacite rocks for manufacturing cutting tools (Darras et al. 2017). This might indicate that the advantages of living on rocky substrates were greater than the fear of volcanic activity. It is also possible that the *Uacúsechas* learned to live in the nearby surroundings, despite of an ongoing eruption, and returned to the Malpaís de Zacapu, once the activity had ceased. In short, the details of the human displacement at the end of the Milpillas phase remain to be elucidated. The emplacement duration, eruptive style, and magnitude described above for the Malpaís de Zacapu volcanoes can aid to mitigate the impact of future eruptions in the MGVF, which is still densely inhabited (Fig. 3h; see also main cities in Fig. 1).

Conclusions

The Malpaís de Zacapu is a Late Holocene volcanic cluster of volcanoes formed by four different monogenetic eruptions, which experienced a complex eruptive history that could be deciphered after extensive sampling for chemical whole-rock and mineral analyses together with radiocarbon and paleomagnetic dating (Mahgoub et al. 2018; Reyes-Guzmán et al. 2018) efforts. In addition, detailed morphological analyses of the flow fields made from high-resolution LiDAR topography, and determination of thermo-rheological parameters (temperature, viscosity) allowed us to reconstruct the dynamics and magnitude of each of the four eruptions and to put some constraints on their possible impact on ancient human populations inhabiting this area.

Our study revealed that the first eruption dated at 1490–1380 BC (Mahgoub et al. 2018; Reyes-Guzmán et al. 2018) initiated in a Strombolian fashion that produced the Las Vigas scoria cone, before turning effusive and emplacing the Infiernillo lava flows. The three subsequent eruptions were largely effusive and include Malpaís Las Víboras (1340–940 BC), El Capaxtiro (200–80 BC), and Malpaís Prieto (~ AD 900; Mahgoub et al. 2018). Together, their lava flows covered an area of 38 km^2 with a volume of ~ 4.4 km^3. Lava viscosities (syn-eruptive conditions) ranged between 4.7×10^4 Pa·s (for the Infiernillo) and 1.4×10^6 Pa·s (for the Malpaís Prieto), while the apparent flow viscosities varied from 10^8 to 10^{11} Pa·s. Accordingly, emplacement duration is estimated at less than a year for Infiernillo, around 3 years for Malpaís Las Víboras and Malpaís Prieto, while the Capaxtiro flow field, which is much more voluminous, could have taken around 27 years to be emplaced. Only the Infiernillo eruption presented a brief initial explosive Strombolian phase, while the other eruptions were almost purely effusive.

These eruptions were not catastrophic. However, continuous tremor and the destruction of arable land during the AD 900 Malpaís Prieto eruption probably forced the massive abandonment of nearby urban sites that had been erected in preceding centuries on the surfaces of the contiguous older Capaxtiro and Infiernillo lava flows. Future collaborative studies between archaeologists and volcanologists might reveal interesting details in terms of human reaction and the development of resilience strategies that might be useful for delineating future civil protections plans.

Supplementary Information The online version contains supplementary material available at https://doi.org/10.1007/s00445-021-01449-0.

Acknowledgments We kindly thank archaeologists O. Quezada and V. Darras for advice in regard to archaeological questions, and E.R. Jiménez for help with equations used for calculating the propagation of uncertainty when following the morphological viscosity-estimate approach. Constructive critical comments by two anonymous journal reviewers and editor H.R. Dietterich were very helpful for making further improvements to the original manuscript.

Funding This work was financed by projects DGAPA-PAPIIT IN103618 and IN104221 granted to C. Siebe. N. Reyes-Guzmán was financed by a CONACYT graduate fellowship (2017–2019), while O.M. Chevrel was financed by a DGAPA-UNAM postdoctoral fellowship. G. Pereira's archaeological investigations were financed by the Uacusecha Archaeological Project (Ministère de l'Europe et des Affaires Etrangères of France and CNRS) and the ANR Mesomobile project. LIDAR data were collected in 2015 by the National Center for Airborn Laser Mapping (NCALM, University of Houston) employing a Teledyne Optech Titan MW multispectral lidar mounted on a Piper Chieftain (PA-31–350) aircraft covering an area of 91.3 km^2. The operation was coordinated by J.C. Fernández-Díaz (NCALM, University of Houston).

References

Albert H, Larrea P, Costa F, Widom E, Siebe C (2020) Crystals reveal magma convection during melt transport in dike-fed eruptions. Sci Rep 10(1):Article 11632 1-10. https://doi.org/10.1038/s41598-020-68421-4

Arnauld C, Faugère-Kalfon B (1998) Evolución de la ocupación humana en el centro-norte de Michoacán (Proyecto Michoacán, CEMCA) y la emergencia del Estado Tarasco. In: Darras V (ed) Génesis, culturas y espacios en Michoacán. CEMCA, México, pp 13–34

Arnauld C, Carot P, Fauvet-Berthelot MF (1993) Arqueología de las Lomas en la Cuenca Lacustre de Zacapu, Michoacán, México. Cuadernos de Estudios Michoacanos 5. Centro de Estudios Mexicanos y Centramericanos, México, p 230

Beattie P (1993) Olivine-melt and orthopyroxene-melt equilibria. Contrib Mineral Petrol 115:103–111

Brey GP, Köhler T (1990) Geothermobarometry in four-phase lherzolites II. New thermobarometers, and practical assessment of existing thermobarometers. J Petrol 31:1353–1378

Carmichael ISE (2002) The andesite aqueduct: perspectives on the evolution of intermediate magmatism in west-central (105° - 99° W) Mexico. Contrib Min Petrol 143(6):641–663

Carr BB, Clarke AB, Vanderkluysen L (2019) Arrowsmith JR (2019) Mechanisms of lava flow emplacement during an effusive eruption of Sinabung Volcano (Sumatra, Indonesia). J Volcanol Geotherm Res 382:137–148. https://doi.org/10.1016/j.jvolgeores.2018.03.002
Carrasco-Núñez G (1997) Lava flow growth inferred from morphometric parameters: a case study of Citlaltepetl volcano. Mexico Geol Mag 134(2):151–162
Cas RAF, Wright JV (1988) Volcanic sucessions: modern and ancient. xviii, London, Boston, Sydney, Wellington, Allen & Unwin, pp. 528
Cashman KV, Thornber C, Kauahikaua JP (1999) Cooling and crystallization of lava in open channels, and the transition of pāhoehoe lava to ʻaʻā. Bull Volcanol 61:306–323. https://doi.org/10.1007/s004450050299
Castruccio A, Rust AC, Sparks RSJ (2013) Evolution of crust- and core-dominated lava flows using scaling analysis. Bull Volcanol 75:681. https://doi.org/10.1007/s00445-012-0681-2
Chevrel MO, Platz T, Hauber E, Baratoux D, Lavallée Y, Dingwell DB (2013) Lava flow rheology: a comparison of morphological and petrological methods. Earth Planet Sci Lett 384:102–120. https://doi.org/10.1016/j.epsl.2013.09.022
Chevrel MO, Guilbaud M-N, Siebe C (2016a) The AD 1250 effusive eruption of El Metate shield volcano (Michoacán, Mexico): magma source, crustal storage, eruptive dynamics, and lava rheology. Bull Volcanol 78(4):1–32. https://doi.org/10.1007/s00445-016-1020-9
Chevrel MO, Guilbaud M-N, Siebe C, Salinas S (2016b) The AD 1250 El Metate shield volcano (Michoacán): Mexico´s most voluminous Holocene eruption and its significance for archaeology and hazards. The Holocene 26(3):471–488
Cigolini C, Borgia A, Casertano L (1984) Intra-crater activity, ʻaʻā-block lava, viscosity and flow dynamics: Arenal Volcano, Costa Rica. J Volcanol Geotherm Res 20:155–176. https://doi.org/10.1016/0377-0273(84)90072-6
Crisp J, Cashman KV, Bonini JA, Hougen SB, Pieri DC (1994) Crystallization history of the 1984 Mauna Loa lava flow. J Geophys Res 99:7177. https://doi.org/10.1029/93JB02973
Darras V (1998) Génesis, culturas y espacios en Michoacán. Centro de Estudios Centroamericanos, México, p 142
Darras V, Mireles C, Siebe C, Quezada O, Castañeda A, Reyes-Guzmán N (2017) The other stone: Dacite quarries and workshops in the Tarascan prehispanic territory, Michoacán. México J Archaeol Sci Rep 12(4):219–231. https://doi.org/10.1016/j.jasrep.2017.01.034
Deardorff ND, Cashman KV (2012) Emplacement conditions of the c. 1,600-year BP Collier Cone lava flow, Oregon: a LiDAR investigation. Bull Volcanol 74:2051–2066
Deligne NI, Conrey RM, Cashman KV, Champion DE, Amidon WH (2016) Holocene volcanism of the upper McKenzie River catchment, central Oregon Cascades, USA. Geol Soc Amer Bull 128(11–12):1618–1635
Dietterich HR, Downs DT, Stelten ME, Zahran H (2018) Reconstructing lava flow emplacement histories with rheological and morphological analyses: the Harrat Rahat volcanic field, Kingdom of Saudi Arabia. Bull Volcanol 80:1–23
Dorison A (2019) Archéologie des systèmes agraires préhispaniques de la région de Zacapu, Michoacán, Mexique, VIIe-XVe siècle apr. J.- C. PhD dissertation, Paris: Université Paris 1 Panthéon-Sorbonne
Faugère BC (2006) Cueva de los Portales. Un sitio arcaico del norte de Michoacán, México. INAH/CEMCA, México, pp. 288
Favalli M, Fornaciai A, Mazzarini F, Harris A, Neri M, Behncke B, Pareschi MT, Tarquini S, Boschi E (2010) Evolution of an active lava flow field using a multi-temporal LIDAR acquisition. J Geophys Res 115 (B1120): 1–17. https://doi.org/10.1029/2010JB007463
Fisher CT (2005) Demographic and landscape change in the lake Pátzcuaro basin, Mexico: abandoning the garden. Amer Anthropol 107(1):87–95
Forest M (2014) Approches spatio-archéologiques de la structure sociale des sites urbains du Malpaís de Zacapu. PhD dissertation, Paris: Université de Paris 1- Panthéon/Sobornne, 595 pp
Forest M, Costa L, Combey A, Dorison A, Pereira G (2019) Testing Web mapping and active learning to approach lidar data. Adv Archaeol Pract 8(1):25–39
Fries C (1953) Volumes and weights of pyroclastic material, lava and water erupted by Parícutin volcano, Michoacán. Mexico Trans Am Geophys Union 34(4):603–616
Gadow H (1930) Jorullo. The history of the volcano of Jorullo and the reclamation of the devastated district by animals and plants. Cambridge University Press, London, pp. 100
Giordano D, Russell JK, Dingwell DB (2008) Viscosity of magmatic liquids: a model. Earth Planet Sci Lett 271:123–134
Gonnermann HM, Manga M (2012) Dynamics of magma ascent in the volcanic conduit. In: Fagents SA, Gregg TKP, Lopes RMC (eds) Modeling volcanic processes. Cambrigde University Press, London, pp 55–84
Guilbaud M-N, Siebe C, Salinas S (2009) Excursions to Paricutin and Jorullo (Michoacán), the youngest volcanoes of the Trans-Mexican Volcanic Belt. A commemorative fieldtrip on the occasion of the 250th anniversary of Volcán Jorullo's birthday on September 29, 1759. México: Impretei S.A., 31 p
Gregg TKP, Fink JH (2000) A laboratory investigation into the effects of slope on lava flow morphology. J Volcanol Geother Res 96:145–159
Griffiths RW (2000) The dynamics of lava flows. Annu Rev Fluid Mech 32:377–518. https://doi.org/10.1146/annurev.fluid.32.1.477
Griffiths RW, Fink JH (1992) The morphology of lava flows in planetary environments: Predictions from analog experiments. J Geophys Res 97(B13):19739. https://doi.org/10.1029/92JB01953
Guest JE, Kilburn CRJ, Pinkerton H, Duncan AM (1987) The evolution of lava flow-fields: observations of the 1981 and 1983 eruptions of Mount Etna, Sicily. Bull Volcanol 49(3):527–540
Guilbaud M-N, Siebe C, Layer P, Salinas S, Castro-Govea R, Garduño-Monroy VH, Le Corvec N (2011) Geology, geochronology, and tectonic setting of the Jorullo Volcano region, Michoacán, México. J Volcanol Geoth Res 201:97–112. https://doi.org/10.1016/j.jvolgeores.2010.09.005
Guilbaud M-N, Siebe C, Layer P, Salinas S (2012) Reconstruction of the volcanic history of the Tacámbaro-Paruarán area (Michoacán, México) reveals high frecuency of Holocene monogenetic eruptions. Bull Volcanol 74(5):1187–1211. https://doi.org/10.1007/s00445-012-0594-0
Guilbaud M-N, Siebe C, Widom E, Rasoazanamparany C, Salinas S, Castro-Govea R (2019) Petrographic, geochemical, and isotopic (Sr-Nd-Pb-Os) study of Plio-Quaternary volcanics and the Tertiary basement in the Jorullo-Tacámbaro area, Michoacán-Guanajuato Volcanic Field. México J Petrol 60(12):2317–2338. https://doi.org/10.1093/petrology/egaa006
Harris AJL, Flynn LP, Matias O, Rose WI, Cornejo J (2004) The evolution of an active silicic lava flow field: an ETM + perspective. 135: 147–168. https://doi.org/10.1016/j.jvolgeores.2003.12.011
Harris AJL, Rowland SK (2009) In: Hoskuldsson A, Thondarson T, Larse G, Self S, Rowland S (Eds.) Effusion rate controls on lava flow length and the role of heat loss: A review. Leg. Georg. P.L. Walker, Spec Publ IAVCEI Geol Soc Lon (2): 33–51
Harris AJL, Rowland SK (2015) Lava flows and rheology. In: Sigurdsson H, Houghton BF, McNutt SR, Rymer H, Stix J (eds) Encyclopedia of volcanoes, 2nd edn. Academic Press, London, pp 321–341

Hasenaka T (1994) Size, distribution, and magma output rate for shield volcanoes of the Michoacan-Guanajuato volcanic field, Central Mexico. J Volcanol Geoth Res 63:13–31
Hasenaka T, Carmichael ISE (1985a) A compilation of location, size, and geomorphological parameters of volcanoes of the Michoacan-Guanajuato volcanic field, central Mexico. Geofis Intern 24(4):577–607
Hasenaka T, Carmichael ISE (1985b) The cinder cones of Michoacán-Guanajuato, Central Mexico: Their age, volume and distribution, and magma discharge rate. J Volcanol Geoth Res 25:105–124
Hasenaka T, Carmichael ISE (1987) The cinder cones of Michoacan-Guanajuato, Central Mexico: Petrology and chemistry. J Petrol 28:241–269
Hulme G (1974) The interpretation of lava flow morphology. Geophys J Roy Astr Soc 39:361–383
Hulme G, Fielder G (1977) Effusion rates and rheology of Lunar lavas. Philos Trans R Soc Lond S-A 285(1327)
INEGI (2020) Instituto Nacional de Geografía, Estadística e Informática website
James MR, Lane SJ, Houghton BF (2012) Unsteady explosive activity: strombolian eruptions. In: Fagents SA, Gregg TKP, Lopes RMC (eds) Modeling volcanic processes. Cambrigde University Press. 107–128
Jeffreys H (1925) The flow of water in an inclined channel of rectangular section. Philos Mag Series 6 49(293):793–807
Kilburn C (2010) Lava flows and flow fields. In: Sigurdsson H, Houghton BF, McNutt SR, Rymer H, Stix J (eds) Encyclopedia of volcanoes. Academic Press, San Diego, pp 291–306
Kilburn CRJ, Lopes R (1991) General patterns of flow field growth: Aa and blocky lavas. J Geophys Res 96(B12 19):721–732
Kolzenburg S, Jaenicke J, Münzer U, Dingwell DB (2018) The effect of inflation on the morphology-derived rheological parameters of lava flows and its implications for interpreting remote sensing data – a case study on the 2014/2015 eruption at Holuhraun, Iceland. J Volcanol Geotherm Res 357:200–212. https://doi.org/10.1016/j.jvolgeores.2018.04.024
Krauskopf KB (1948) Lava movement at Paricutin volcano. Mexico Geol Soc Am Bull 59(12):1267–1284
Kshirsagar P, Siebe C, Guilbaud M-N, Salinas S (2016) Geological and environmental controls on the change of eruptive style (phreatomagmatic to Strombolian-effusive) of Late Pleistocene El Caracol tuff cone and its comparison with adjacent volcanoes around the Zacapu basin (Michoacán, México). J Volcanol Geoth Res 318:114–133. https://doi.org/10.1016/j.jvolgeores.2016.03.015
Larrea P, Albert H, Ubide T, Costa F, Colás V, Widom E, Siebe C (2021) From explosive vent opening to effusive outpouring: mineral micro-analytical constraints on magma dynamics and timescales at Paricutin monogenetic volcano. J Petrol. https://doi.org/10.1093/petrology/egaa112
Larrea P, Salinas S, Widom E, Siebe C, Abbitt RJF (2017) Compositional and volumetric development of a monogenetic lava flow field: the historical case of Paricutin (Michoacán, Mexico). J Volcanol Geoth Res 348:36–48. https://doi.org/10.1016/j.jvolgeores.2017.10.016
Larrea P, Siebe C, Juárez-Arriaga E, Salinas S, Ibarra H, Böhnel H (2019a) The ~AD 500–700 (Late Classic) El Astillero and El Pedregal volcanoes (Michoacán, Mexico): a new monogenetic cluster in the making? Bull Volcanol 81(10):59. https://doi.org/10.1007/s00445-019-1318-5
Larrea P, Widom E, Siebe C, Salinas S, Kuentz D (2019b) A re-interpretation of the petrogenesis of Paricutin volcano: Distinguishing crustal contamination from mantle heterogeneity. Chem Geol 504:66–82. https://doi.org/10.1016/j.chemgeo.2018.10.026
Laturrie B, Harris A, Médard E, Gurioli L (2017) Eruption and emplacement dynamics of a thick trachytic lava flow of the Sancy volcano (France). Bull Volcanol 79(1):1–21. https://doi.org/10.1007/s00445-016-1084-6
Lavallée Y, Hess KU, Cordonnier B, Dingwell DB (2007) Non-Newtonian rheological law for highly crystalline dome lavas. Geology 35:843–846
LeBas MJ, Le Maitre RW, Streckeisen A, Zanettin B (1986) A chemical classification of volcanic rocks based on the total alkali– silica diagram. J Petrol 27:745–750
Lipman PW, Banks NG (1987) A flow dynamics, Mauna Loa 1984. US Geol Surv Prof Pap 1350:1527–1567
Lipman PW, Banks NG, Rhodes JM (1985) Degassing-induced crystallization of basaltic magma and effects on lava rheology. Nature 317:604–607
Mader HM, Llewellin EW, Muller SP (2013) The rheology of two-phase magmas: A review and analysis. J Volcanol Geoth Res 257:135–158
Mahgoub AN, Böhnel H, Siebe C, Chevrel MO (2017a) Paleomagnetic study of El Metate shield volcano (Michoacán, Mexico) confirms its monogenetic nature and young age (~1250 CE). J Volcanol Geoth Res 336:209–218. https://doi.org/10.1016/j.jvolgeores.2017.02.024
Mahgoub AN, Böhnel H, Siebe C, Salinas S, Guilbaud M-N (2017b) Paleomagnetically inferred ages of a cluster of Holocene monogenetic eruptions in the Tacámbaro-Puruarán area (Michoacán, México): implications for volcanic hazards. J Volcanol Geoth Res 347:360–370. https://doi.org/10.1016/j.jvolgeores.2017.10.004
Mahgoub AN, Reyes-Guzmán N, Böhnel H, Siebe C, Pereira G, Dorison A (2018) Paleomagnetic constraints on the ages of the Holocene Malpaís de Zacapu lava flow eruptions, Michoacán (Mexico): implications for archeology and volcanic hazards. Holocene 8(2):220–245. https://doi.org/10.1177/0959683617721323
Maron SH, Pierce PE (1956) Application of Ree-Eyring generalized flow theory to suspensions of spherical particles. J Colloid Sci 11:80–95
Mazzarini F, Pareschi MT, Favalli M, Isola I, Tarquini S, Boschi E (2007) Lava flow identification and aging by means of lidar intensity: Mount Etna case. J Geophys Res 112:B02201
Michelet D (1992) El Centro-Norte de Michoacán: características generales de su estudio regional. El Proyecto Michoacán 1983–1987. Medio ambiente e introducción a los trabajos arqueológicos. CEMCA, México, pp 9–52
Michelet D, Arnauld MC, Fauvet-Berthelot MF (1989) El Proyecto del CEMCA en Michoacán. Etapa I. Un balance TRACE 16:70–87
Michelet D, Pereira G, Migeon G (2005) La llegada de los Uacúsechas a la región de Zacapu, Michoacán: Datos arqueológicos y discusión. In: Manzanilla L (ed) Reacomodos demográficos del Clásico al Posclásico en el centro de México. UNAM, México, pp 137–153
Moore HJ (1987) Preliminary estimates of the theological properties of 1984 Mauna Loa lava. US Geol Surv Prof Pap 1350(99):1569–1588
Muller S, Llewellin EW, Mader HM (2010) The rheology of suspensions of solid particles. Trans R Soc Lond A 466:1201–1228
Naranjo JA, Sparks RSJ, Staslu MV, Moreno H, Ablay GJ (1992) Morphological, structural and textural variations in the 1988–1990 andesite lava of Loquimay volcano. Chile Geol Mag 12(6):657–678
Navarro-Ochoa C, Gavilanes-Ruiz JC, Cortes-Cortes A (2002) Movement and emplacement of lava flows at Volcan de Colima, Mexico: November 1998-Frebuary 1999. J Vol Geoth Resea 117:155–167

Neave D, Putirka D (2017) A new clinopyroxene-liquid barometer, and implications for magma storage pressures under Icelandic Rift Zones. Amer Mineral 102(4):777–794
Nichols RL (1939) Viscosity of lava. J Geol 47:290–302
Nolan ML, Gutiérrez C (1979) Impact of Paricutin on five communities. In: Sheets, P.D. and Grayson, D.K. (edits.), Volcanic Activity and Human Ecology. Academic Press, New York, p 293–338
Pétrequin P (1994) 8000 años de la cuenca de Zacapu. Centre de Etudes Mexicaines et Centramericaines, Mexico. Cuadernos de Estudios Michoacanos 6: 144 pp.
Pereira G, Forest M, Jadot E, Darras V (2021) Ephemeral cities? The longevity of the Postclassic Tarascan urban sities of Zacapu Malpaís and its consequences on the migration process. In: Arnauld, M.C., Beekman, C., Pereira G. (eds), Mobility and Migration in Ancient Mesoamerican Cities. University Press of Colorado, Boulder, pp 208–231
Phan-Thien N, Pham DC (1997) Differential multiphase models for polydispersed suspensions and particulate solids. J Nonnewton Flud Mech 72:305–318
Pinkerton H, Sparks RSJ (1976) The 1975 sub-terminal lavas, Mount Etna: a case history of the formation of a compound lava field. J Volcanol Geoth Res 1:167–182
Pinkerton H, Wilson L (1994) Factors controlling the lengths of channel-fed lava flows. J Volcanol Geoth Res 56:108–120
Putirka KD (2008) Thermometers and barometers for volcanic systems. Rev Mineral Geochem 69:61–120
Putirka K, Johnson M, Kinzler R, Walker D (1996) Thermobarometry of mafic igneous rocks based on clinopyroxene-liquid equilibria, 0–30 kbar. Contrib Mineral Petrol 123:92–108
Ramírez-Uribe I, Siebe C, Chevrel MO, Fisher CT (2021) Rancho Seco monogenetic volcano (Michoacán, Mexico): Petrogenesis and lava flow emplacement based on LiDAR images. J Volcanol Geoth Res. https://doi.org/10.1016/j.jvolgeores.2020.107169
Ramírez-Uribe I, Siebe C, Salinas S, Guilbaud M-N, Layer P, Benowitz J (2019) 14C and 40Ar/39Ar radiometric dating and geologic setting of young lavas of Rancho Seco and Mazcuta volcanoes hosting archaeological sites at the margins of the Pátzcuaro and Zacapu lake basins (central Michoacán, Mexico). J Volcanol Geoth Res 388:1–22. https://doi.org/10.1016/j.jvolgeores.2019.106674
Reyes-Guzmán N, Siebe C, Chevrel MO, Guilbaud M-N, Salinas S, Layer P (2018) Geology and radiometric dating of Quaternary monogenetic volcanism in the western Zacapu lacustrine basin (Michoacán, México): implications for archeology and future hazard evaluations. Bull Volcanol 80(2):18. https://doi.org/10.1007/s00445-018-1193-5
Rowland SK, Jurado-Chichay Z, Ernst G, Walker GPL (2009) Pyroclastic deposits and lava flows from the 1759–1774 eruption of El Jorullo, México: aspects of 'violent Strombolian' activity and comparision with Parícutin. In: Thordarson T, Self S, Larsen G, Rowland SK, Hoskuldsson A (eds) Studies in Volcanology: The legacy of George Walker. Geological Society, London, 2, p 105–128, Special Publications of IAVCEI
Tarquini S, de Michieli Vitturi M (2014) Influence of fluctuating supply on the emplacement dynamics of channelized lava flows. Bull Volcanol 76. https://doi.org/10.1007/s00445-014-0801-2
Tarquini S, Favalli M, Mazzarini F, Isola I, Fornaciai A (2012) Morphometric analysis of lava flow units: Case study over LIDAR-derived topography at Mount Etna. Italy J Volcanol Geoth Res 235–236:11–22. https://doi.org/10.1016/j.jvolgeores.2012.04.026
Walker GPL (1973) Lengths of lava flows. Philos Trans R Soc Lond 274:107–118
Watts WA, Bradbury JP (1982) Paleoecological studies at Lake Patzcuaro on the west-central Mexican Plateau and at Chalco in the Basin of Mexico. Quat Res 17(1):56–70
Water LE, Lange RA (2015) An updated calibration of the plagioclase liquid hygrometer-thermometer applicable to basalts through rhyolites. Am Min 100: 2172-2184
Wilcox RE (1954) Petrology of Paricutin Volcano, Mexico. US Geol Surv Bull 965C:281–353
Wilson L, Head JW (1983) A comparison of volcanic eruption processes on Earth, Moon, Mars, Io and Venus. Nature 302:663–669
Younger ZP, Valentine GA, Gregg TKP (2019) 'A'a lava emplacement and the significance of rafted pyroclastic material: Marcath volcano (Nevada, USA). Bull Volcanol 81(9):50–65